



UNIVERSIDADE ESTADUAL DE MARINGÁ  
CENTRO DE CIÊNCIAS BIOLÓGICAS  
PROGRAMA DE PÓS GRADUAÇÃO EM CIÊNCIAS BIOLÓGICAS  
ÁREA DE CONCENTRAÇÃO: BIOLOGIA CELULAR E MOLECULAR

## **EFEITOS DO ANTIMICROBIANO TRICLOCARBAN SOBRE O METABOLISMO HEPÁTICO DE RATO**

**VANESA DE OLIVEIRA PATEIS**

**Maringá  
2022**

**VANESA DE OLIVEIRA PATEIS**

**EFEITOS DO ANTIMICROBIANO TRICLOCARBAN  
SOBRE O METABOLISMO HEPÁTICO DE RATO**

Tese apresentada ao Programa de Pós-graduação em Ciências Biológicas (Área de concentração - Biologia Celular e Molecular) da Universidade Estadual de Maringá para obtenção do grau de Doutor em Ciências Biológicas.

**Orientador: Prof. Dr.  
Jurandir Fernando Comar**

**Maringá  
2022**

Dados Internacionais de Catalogação-na-Publicação  
(CIP)(Biblioteca Central - UEM, Maringá - PR,  
Brasil)

P295e

Pateis, Vanesa de Oliveira

Efeitos do antimicrobiano triclocarban sobre o metabolismo hepático de rato / Vanesa de Oliveira Pateis. -- Maringá, PR, 2022.  
76 f.: il. color., figs., tabs.

Orientador: Prof. Dr. Jurandir Fernando Comar.

Tese (Doutorado) - Universidade Estadual de Maringá, Centro de Ciências Biológicas, Departamento de Bioquímica, Programa de Pós-Graduação em Ciências Biológicas (Biologia Celular), 2022.

1. Metabolismo hepático. 2. Triclocarban. 3. Antimicrobiano. 4. Perfusão hepática. 5. Gliconeogênese. I. Comar, Jurandir Fernando, orient. II. Universidade Estadual de Maringá. Centro de Ciências Biológicas. Departamento de Bioquímica. Programa de Pós-Graduação em Ciências Biológicas (Biologia Celular). III. Título.

CDD 23.ed. 572.4

Elaine Cristina Soares Lira - CRB-  
9/1202

**VANESA DE OLIVEIRA PATEIS**

**EFEITOS DO ANTIMICROBIANO TRICLOCARBAN SOBRE O  
METABOLISMO HEPÁTICO DE RATO**

Tese apresentada ao Programa de Pós-graduação em Ciências Biológicas (Área de concentração - Biologia Celular e Molecular) da Universidade Estadual de Maringá, para obtenção do grau de Doutor em Ciências Biológicas.

Aprovado em: 16/09/2022

**BANCA EXAMINADORA**

---

Prof<sup>o</sup> Dr<sup>o</sup> Jurandir Fernando Comar (orientador)  
Universidade Estadual de Maringá

---

Prof<sup>a</sup> Dr<sup>a</sup> Alexandra Acco  
Universidade Federal do Paraná

---

Prof<sup>a</sup> Dr<sup>a</sup> Anacharis Babeto de Sá-Nakanishi (Presidente)  
Universidade Estadual de Maringá

---

Prof<sup>a</sup> Dr<sup>a</sup> Rodrigo Polimeni Constantin  
Universidade Estadual de Maringá

---

Prof<sup>a</sup> Dr<sup>a</sup> Maria Ida Bonini Ravanelli Speziali  
Universidade Estadual de Maringá

## **BIOGRAFIA**

Vanessa de Oliveira Pateis nasceu em Maringá/PR em 03/09/1990. Possui graduação em Bioquímica Bacharelado pela Universidade Estadual de Maringá (2014) e mestrado em Ciências Biológicas (Área de concentração – Biologia Celular e Molecular) pela Universidade Estadual de Maringá UEM (2017).

## **AGRADECIMENTOS**

Gostaria de agradecer em primeiro lugar à Deus, que me permitiu chegar até aqui, sem a benção dele nada seria possível. Agradeço, também, a minha família, meus pais que sempre me apoiaram nos meus estudos e não mediram esforços para me proporcionar uma educação de qualidade. Agradeço meu marido, que também me apoiou muito nos momentos de correria do doutorado, e também a meu filho, que apesar de pequeno, sempre entendeu quando eu tinha que trabalhar ou estudar.

Por fim, agradeço a todos os membros do Laboratório de Metabolismo Hepático, que me acolherem muito bem desde o início do meu mestrado, em especial ao meu orientador Dr Jurandir F. Comar, que aceitou me orientar. As professoras Dra Anacharis Babeto de Sá Nakanishi e a Dra Lívia Bracht, que sempre estão dispostas a ajudar no nosso dia a dia do laboratório.

Não poderia deixar de agradecer, também, à Capes, que me financiou todo esse período, e sem esse benefício não conseguiria concluir meu Doutorado.

## APRESENTAÇÃO

O presente trabalho foi realizado no Laboratório de Metabolismo Hepático do Departamento de Bioquímica da Universidade Estadual de Maringá. A apresentação está na forma de dois artigos científicos originais, em consonância com as regras do Programa de Pós-graduação em Ciências Biológicas.

Artigo 1:

Pateis, V.O; Bracht, L; Bracht, A.; Comar, J.F. **Short-term effects of the antimicrobial agent triclocarban on the energetic metabolism of rat liver.** SERÁ submetido ao Toxicol Appl Pharmacol (Cite score 7.1/Impact Fator 4,46).

Artigo 2:

Pateis, V.O; Ames-Sibin, A.P.; Bracht, L; Bracht, A.; Comar, J.F. **Effects of triclocarban on the energetic content and gluconeogenic enzymes activity in the rat liver.** SERÁ submetido ao Cell Biochem Funct (Impact Fator 3,963).

## RESUMO

**INTRODUÇÃO E OBJETIVOS:** O triclocarban (TCC) é um composto aromático policlorado usado como antimicrobiano em vários produtos de higiene pessoal, em ambientes médicos e mesmo incorporados a plásticos. Este composto é absorvido pela mucosa oral e pele e é encontrado em fluidos humanos, incluindo urina, sangue e fluido seminal. O TCC está associado à desregulação endócrina e resistência bacteriana, mas muitos efeitos são ainda controversos e requerem pesquisas adicionais. O fígado está envolvido em várias funções fisiológicas, incluindo um papel central na homeostase metabólica corporal. Por outro lado, o TCC é metabolizado pelo citocromo P450 no fígado e pode afetar o metabolismo hepático. De fato, o TCC modifica negativamente a respiração de mitocôndrias isoladas de fígado de rato por um mecanismo que envolve um desacoplamento da fosforilação oxidativa. Análises de metabolômica revelam que o TCC administrado oralmente em camundongos causa hepatotoxicidade e modifica o metabolismo hepático por mecanismos que envolvem aceleração da gliconeogênese e inibição da glicólise aeróbica. A gliconeogênese, no entanto, não deveria ser aumentada se a fosforilação oxidativa mitocondrial estiver desacoplada e a produção de ATP for reduzida no fígado. Considerando que os efeitos do TCC sobre a gliconeogênese e outras vias metabólicas no fígado ainda são controversos, este estudo investigou as ações de curto prazo do TCC sobre a gliconeogênese, detoxificação de amônia e catabolismo do glicogênio em fígados de rato. As ações do TCC sobre a respiração e atividade das enzimas NADH e succinato oxidases foram avaliadas em mitocôndrias hepáticas isoladas. Foram também quantificados os conteúdos de ATP, ADP e AMP em fígados perfundidos e atividade de enzimas-chave gliconeogênicas. As transformações de passagem única do TCC foram avaliadas em fígados perfundidos.

**MÉTODOS:** O fígado de rato em perfusão isolada com tampão Krebs/Henseleit (pH 7,4) foi utilizado como ferramenta experimental. TCC em concentrações de até 75  $\mu\text{M}$  foram introduzido no fígado perfundido. O catabolismo do glicogênio foi avaliado em fígados de ratos alimentados e a gliconeogênese em fígados de ratos em jejum de 15 h usando lactato (2,0 mM), alanina (2,5 mM) e frutose (2,5 mM) como precursores. Amostras do fluido de perfusão efluente foram coletadas em intervalos regulares e analisadas quanto ao conteúdo de glicose, lactato, piruvato, uréia e amônia por espectrofotometria e TCC foi quantificado

por HPLC. O consumo hepático de oxigênio foi monitorado por polarografia. Os conteúdos de ATP, ADP e AMP foram determinados por HPLC. A respiração e as atividades das enzimas NADH- e succinato oxidases foram determinadas em mitocôndrias hepáticas isoladas por polarografia. A atividade da glicose 6-fosfatase (G6Pase), fosfoenolpiruvato carboxiquinase (PEPCK) e frutose 1,6-bisfosfatase (FBPase-1) foi determinada em microsomos por espectrofotometria e a carboxilação do piruvato foi determinada em mitocôndrias acopladas por cintilação líquida usando  $[^{14}\text{C}]\text{NaHCO}_3$ . A significância estatística dos dados foi analisada por ANOVA ONE-WAY e aplicado o teste post-hoc de Newman-Keuls ( $p < 0,05$ ). As concentrações de TCC que induzem metade da estimulação ( $\text{EC}_{50}$ ) ou inibição ( $\text{IC}_{50}$ ) máximos foram calculados por interpolação numérica, com o Programa Scientist.

**RESULTADOS E DISCUSSÃO:** Em termos gerais, o TCC diminuiu os processos anabólicos e aumentou os fluxos catabólicos no fígado. Mais especificamente, o TCC inibiu a custosa gliconeogênese a partir dos três substratos testados: lactato ( $\text{IC}_{50} = 17,5 \mu\text{M}$ ), alanina ( $\text{IC}_{50} = 14,5 \mu\text{M}$ ) e frutose ( $\text{IC}_{50} = 21,4 \mu\text{M}$ ). O TCC também diminuiu a detoxificação da amônia ( $\text{IC}_{50} = 19,1 \mu\text{M}$ ). A inibição destas vias foi acompanhada de um estímulo do consumo de oxigênio hepático. A combinação de ambas inibição destas vias e estímulo do consumo de oxigênio, é esperada para um inibidor da transdução de energia mitocondrial que atua principalmente como um desacoplador. A glicólise ( $\text{EC}_{50} = 6,9 \mu\text{M}$ ) e a frutólise foram estimuladas provavelmente como um fenômeno citosólico compensatório pela diminuição da produção mitocondrial de ATP. A glicogenólise foi estimulada ( $\text{EC}_{50} = 7,0 \mu\text{M}$ ) provavelmente para fornecer glicose 6-fosfato para o aumentado fluxo glicolítico e biotransformação de TCC. Esse processo também foi acompanhado por um estímulo do consumo hepático de oxigênio, fenômeno fortemente inibido pelo cianeto, um inibidor da cadeia de transporte de elétrons mitocondrial, mas não modificado pelo proadifeno, um inibidor do sistema citocromo P450. Isto mostra que o estímulo do consumo de oxigênio causado pelo TCC é provavelmente devido ao aumento da atividade respiratória mitocondrial. No entanto, a respiração de mitocôndrias isoladas apresentou um comportamento complexo. A respiração basal e o estado IV foram inibidos pelo TCC quando alfa-cetoglutarato foi o substrato, com  $\text{IC}_{50}$  de 40,7 e 20,8  $\mu\text{M}$ , respectivamente. Quando o succinato foi o substrato, a respiração basal e o estado IV foram estimulados com  $\text{EC}_{50}$  de 2,4 e 1,9  $\mu\text{M}$ , respectivamente. O

estado III da respiração foi inibido independentemente do substrato (succinato ou alfa-cetoglutarato). A atividade da NADH- e succinato oxidases não foi modificada. Os resultados com mitocôndrias isoladas mostram que, além de um agente desacoplador, o TCC também age como inibidor do fluxo de elétrons acoplado, o que pode ser uma inibição ao nível do complexo ATP sintase. O conteúdo hepático de ATP, ADP e AMP foram determinados em fígados perfundidos sob condição gliconeogênica. O TCC diminuiu o conteúdo hepático de ATP em 38% e aumentou o conteúdo de AMP em 95%. O conteúdo de ADP não foi modificado. O TCC diminuiu as razões ATP/ADP e ATP/AMP respectivamente em 42% e 70%. A redução do aporte energético no fígado deve ser a consequência de uma fosforilação oxidativa mitocondrial prejudicada e é provavelmente a principal razão pela qual o TCC inibe a dispendiosa gliconeogênese e detoxificação de amônia em fígados de ratos perfundidos. O TCC não modificou a atividade hepática da G6Pase, FBPase-1 e PEPCK, entretanto, a carboxilação do piruvato foi inibida pelo composto. Este último, no entanto, foi medido em mitocôndrias acopladas que precisam respirar para produzir o ATP usado na reação. Assim, a inibição da carboxilação do piruvato pode ser causada pelo comprometimento da atividade mitocondrial. A passagem única de TCC 25  $\mu$ M através de fígados perfundidos mostra que o composto é extensivamente retido e/ou transformado no órgão (mais de 90%) e esta porcentagem é mantida ou mesmo aumentada quando TCC 75  $\mu$ M é infundido. Os resultados mostram que a grande redução da carga energética do fígado pode ser devida ao próprio composto retido ou seus metabólitos produzidos.

**CONCLUSÃO:** O estudo apresenta as ações de curto prazo do TCC sobre o fígado e devem contribuir para o entendimento de sua toxicidade aguda. O TCC produz efeitos significativos sobre o metabolismo energético hepático em concentrações portal tão baixas quanto 5  $\mu$ M. Mais especificamente, o TCC inibe a gliconeogênese e impede a detoxificação de amônia no fígado de ratos em perfusão, os quais ocorrem devido principalmente à queda de ATP associada ao metabolismo energético mitocondrial prejudicado. Os resultados com mitocôndrias isoladas mostram que, além de um agente desacoplador, o TCC também inibe a respiração mitocondrial, pois o composto inibiu fluxo de elétrons ao longo da cadeia transposrtadora de elétrons.

**PALAVRAS-CHAVE:** Triclocarban, metabolismo hepático, perfusão hepática, gliconeogênese.

## ABSTRACT

**BACKGROUND AND AIMS:** Triclocarban (TCC) is a polychlorinated aromatic compound used as antimicrobial agent in various personal care products, medical settings and plastics. This biocide is absorbed into oral mucosa and skin and it is found in human fluids, including urine, blood and seminal fluid. TCC has been associated with endocrine disruption and bacterial resistance, but many effects of the compound to humans remain controversial and require additional research. The liver is involved in a number of physiological functions, including a pivotal role in body metabolic homeostasis. On the other hand, TCC is metabolized by cytochrome P450 in the liver and it could affect the hepatic metabolism. In fact, TCC negatively modifies the respiration of rat liver isolated mitochondria by a mechanism that involves an uncoupling of oxidative phosphorylation. Metabolomics analysis reveals that TCC orally administered to mice triggers hepatotoxicity and modifies the liver metabolism by mechanisms that involves an acceleration of gluconeogenesis and inhibition of aerobic glycolysis. Gluconeogenesis, however, could not be increased if mitochondrial oxidative phosphorylation is uncoupled and ATP production is reduced in the liver. Considering that effects of TCC on gluconeogenesis and other metabolic pathways in the liver are still controversial, this study investigated the short-term actions of TCC on gluconeogenesis, ammonia detoxification and glycogen catabolism in the liver of rats. The actions of TCC on the respiratory activity and the of NADH- and succinate oxidates activity were in addition evaluated in isolated hepatic mitochondria. Also the content of ATP, ADP and AMP in perfused livers and hepatic gluconeogenic key enzymes activity *in vitro* were determined. Finally, the single-pass transformations of TCC were accessed in perfused livers.

**METHODS:** The rat livers in isolated perfusion with Krebs/Henseleit buffer (pH 7.4) was used as experimental tool. TCC at concentrations range up to 75  $\mu\text{M}$  were introduced in perfused livers. Glycogen catabolism was evaluated in livers from fed rats and gluconeogenesis in livers of 15 h fasted rats using lactate (2.0 mM), alanine (2.5 mM) and fructose (2.5 mM) as precursors. Samples of the effluent perfusion fluid were collected at regular intervals and analyzed for their content of glucose, lactate, pyruvate, urea and ammonia by spectrophotometry, and TCC by HPLC. Hepatic oxygen uptake was monitored by polarography. The contents of ATP, ADP and AMP were determined in freeze-clamped perfused

livers by HPLC. Respiration and NADH- and succinate oxidases activities were determined in isolated hepatic mitochondria by polarography. The activity of glucose 6-phosphatase (G6Pase), phosphoenolpyruvate carboxykinase (PEPCK) and fructose 1,6-bisphosphatase (FBPase-1) was assayed by spectrophotometry and the carboxylation of pyruvate was assayed in coupled mitochondria by liquid scintillation using  $[^{14}\text{C}]\text{NaHCO}_3$ . The statistical significance of the data was analyzed by means of ANOVA ONE-WAY and the Newman-Keuls post-hoc test was applied ( $p < 0.05$ ). Half-maximum stimulation ( $\text{EC}_{50}$ ) and inhibition ( $\text{IC}_{50}$ ) concentration values were calculated by numerical interpolation.

**RESULTS AND DISCUSSION:** In general terms, TCC diminished anabolic processes and increased catabolic fluxes in the organ. These effects were concentration-dependent in their majority. More specifically, TCC inhibited the costly gluconeogenesis from the all three substrates tested, namely lactate ( $\text{IC}_{50} = 17.5 \mu\text{M}$ ), alanine ( $\text{IC}_{50} = 14.5 \mu\text{M}$ ) and fructose ( $\text{IC}_{50} = 21.4 \mu\text{M}$ ). TCC also impaired the ammonia detoxification ( $\text{IC}_{50} = 19.1 \mu\text{M}$ ) which is also dependent of ATP generated within the mitochondria. The inhibition of gluconeogenesis and ammonia detoxification was accompanied of a stimulus of the liver oxygen consumption. The combination of both inhibition of these costly pathways associated with stimulus of the oxygen consumption is normally expected from an inhibitor of energy transduction in mitochondria that acts mainly as an uncoupler agent. In relation to catabolic process, glycolysis ( $\text{EC}_{50} = 6.9 \mu\text{M}$ ) and fructolysis were stimulated probably as a cytosolic compensatory phenomena for the diminished mitochondrial ATP production. Glycogenolysis was also stimulated ( $\text{EC}_{50} = 7.0 \mu\text{M}$ ) probably to provide glucose 6-phosphate for the increased glycolytic flux and biotransformation of TCC. This process was also accompanied by a stimulus of hepatic oxygen consumption, a phenomenon that was strongly inhibited by cyanide, an inhibitor of mitochondrial electron transport chain, but not modified by proadifen, an inhibitor of the cytochrome P450 system. The latter shows that the stimulus of oxygen consumption was not due to metabolism of TCC, but due to an increased respiratory activity of mitochondria. However, the respiration of isolated mitochondria showed a complex behavior. Basal and state IV respiration were inhibited by TCC when alpha-ketoglutarate was the substrate, with  $\text{IC}_{50}$  of 40.7 and 20.8  $\mu\text{M}$ , respectively. When succinate was the substrate, basal and state IV respiration

were stimulated by TCC with  $EC_{50}$  of 2.4 and 1.9  $\mu\text{M}$ , respectively. State III respiration was inhibited irrespective of the substrate (succinate or  $\alpha$ -ketoglutarate). The activity of NADH- and succinate oxidases were not modified. The results of isolated mitochondria show that in addition to an uncoupler agent TCC also inhibits the coupled electron flow at the mitochondrial level, which could be an inhibition at the level of the complex ATP synthase. The hepatic content of ATP, ADP and AMP were determined in perfused livers under gluconeogenic condition using lactate as precursor. TCC decreased the hepatic content of ATP by 38% and increased the content of AMP by 95%. The ADP content was not modified by TCC in the liver. TCC decreased the ratios of ATP/ADP and ATP/AMP by 42% and 70%, respectively. The reduced energetic apport in the liver must be certainly the consequence of an impaired mitochondrial oxidative phosphorylation and is probably the main reason by which TCC inhibits the costly gluconeogenesis and ammonia detoxification in perfused rat livers. TCC did not modify the liver activity of G6Pase, FBPase-1 and PEPCK, however, the carboxylation of pyruvate was inhibited by the compound. The latter, however, is measured in phosphorylating mitochondria which must to respire to produce the ATP used in the reaction. Thus, the inhibition of pyruvate carboxylation can be caused by the impairment of mitochondrial activity. The single-pass 25  $\mu\text{M}$  TCC through perfused livers shows that the compound is extensively retained and/or transformed in the organ (more than 90%) and this percentage is maintained or even increased when 75  $\mu\text{M}$  TCC is infused. The results show that the great reduction of the energetic load of the liver can be due to the compound itself or its metabolites.

**CONCLUSION:** The study presents the short-term actions of TCC in the liver, which should contribute to understand its acute toxicity. TCC produces significant effects on the hepatic energy metabolism at portal concentrations as low as 5  $\mu\text{M}$ . More specifically, TCC inhibited the liver gluconeogenesis and impaired the ammonia detoxification, which must be the consequence mainly of an impaired mitochondrial energy metabolism. The results of isolated mitochondria show that in addition to an uncoupler agent TCC also inhibits the coupled electron flow at the mitochondrial level, which should be the cause of the impaired gluconeogenesis and hepatotoxicity in the liver.

**KEYWORDS:** *Triclocarban, liver metabolism, liver perfusion, gluconeogenesis.*

# **Short-term effects of the antimicrobial agent triclocarban on the energetic metabolism of rat liver**

Vanesa de Oliveira Pateis<sup>1</sup>, Livia Bracht<sup>1</sup>, Adelar Bracht<sup>1</sup>, Jurandir F. Comar<sup>1\*</sup>

<sup>1</sup> Department of Biochemistry, State University of Maringá, PR, Brazil

Address for correspondence:

\*Jurandir Fernando Comar

Department of Biochemistry

University of Maringá

87020900 Maringá, Brazil

Email: [jfcomar@uem.br](mailto:jfcomar@uem.br)

Grant sponsor: Conselho Nacional de Desenvolvimento Científico e Tecnológico (CNPq); Grant number: 447876/2014-7

## ABSTRACT

Triclocarban (TCC) is a polychlorinated antimicrobial agent extensively used as antiseptic and preservative in personal care products, medical supplies and plastics. TCC orally administered triggers hepatotoxicity in mice and, *in vitro*, it negatively modifies the respiration of isolated hepatic mitochondria. These actions could impair the energy-dependent metabolic fluxes in the liver. Therefore, this study investigated the actions of TCC (5 – 75  $\mu\text{M}$ ) on gluconeogenesis and glycogen catabolism in perfused livers of rats. The actions of TCC were further evaluated on isolated hepatic mitochondria. TCC at concentrations range up to 75  $\mu\text{M}$  was introduced in perfused livers. Glycogen catabolism was evaluated in livers from fed rats and gluconeogenesis in livers of 15 h fasted rats using lactate, alanine and fructose as substrates. Mitochondrial respiration and the activity of NADH- and succinate oxidases were determined by polarography. TCC stimulated the oxygen uptake, fructolysis, and glycogenolysis and glycolysis from glycogen stores in the liver of fed rats. TCC inhibited the glucose production from all substrates tested. The oxygen uptake, however, was stimulated only when fructose (all TCC concentrations) or alanine (only 50  $\mu\text{M}$  TCC) were the substrates. The ammonia and lactate production from alanine was stimulated by TCC while the urea production was decreased. The respiration of isolated mitochondria showed a complex behavior. Basal and state IV respiration were inhibited by TCC when alpha-ketoglutarate was the substrate. When succinate was the substrate, basal and state IV respiration were stimulated by TCC. State III respiration was inhibited irrespective of the substrate (succinate or alpha-ketoglutarate). The activity of NADH- and succinate oxidases were not modified. The results of isolated mitochondria show that in addition to an uncoupler agent TCC also inhibits the coupled electron flow at the mitochondrial level, which should be the cause of the impaired gluconeogenesis and hepatotoxicity in the liver.

**Keywords:** *triclocarban, liver metabolism, liver perfusion, glycogen catabolism, gluconeogenesis, antiseptic, antiseptic*

## 1. INTRODUCTION

Chemical biocides are poisonous substances including preservatives, insecticides, disinfectants, and pesticides used for the control of organisms that are harmful to human or animal health or that cause damage to natural or manufactured products. They have been broadly employed around the world for a wide range applications and environments, including consumer products, wastewater, foods and pharmaceutical industries [Maillard, 2018]. In spite of the stringent regulation in US and Europe, the usage of biocide products is continuing to increase due to their versatility for product preservation and environment disinfection. One concern is that such heavy usage of biocides could be associated with significant adverse effects on the natural environment and human health, particularly increased bacterial cross-resistance to unrelated antibiotics [Maillard, 2018; Hernández-Moreno et al., 2018].

Triclocarban (TCC), 3-(4-chlorophenyl)-1-(3,4-dichlorophenyl)urea, is a synthetic polychlorinated compound extensively used as antibacterial and antifungal agent in various consumer products, including toothpaste, soaps, shampoo, antiperspirants and even plastic and toys [Iacopetta et al., 2021]. The planar structure of TCC is shown in Fig. 1. TCC and its analog triclosan are also used in medical settings as disinfectant and antiseptic agents [Iacopetta et al., 2021]. The precise mechanism of the biocide action of TCC is unknown, however, it has been pointed out to non-specifically adsorb to cell membranes of microorganisms and interrupt their growth [Schebb et al., 2011].

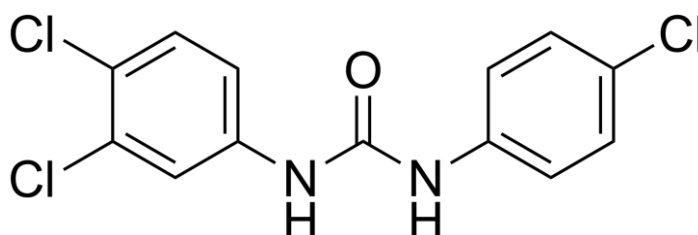


**Fig.1.** Planar structure of triclocarban (TCC).

TCC is quickly absorbed into oral mucosa and skin and it is found in a number of human fluids, including urine, blood and seminal fluid [Halden et al., 2017; Buck Louis et al., 2018; Wei et al., 2017; Yin et al., 2016], drawing attention as a potential risk to human health. In mammals, this biocide has been associated with endocrine disruption and its uncontrolled use has been in

addition related to bacterial resistance [Buck Louis et al., 2018; Halden et al., 2017; Kim & Rhee, 2016]. TCC has been reported to inhibit the human soluble epoxide hydrolase, an enzyme related to regulation of inflammation [Schebb et al., 2011]. The exposure to TCC has been also pointed as a potential risk for colitis [Xie et al., 2020]. TCC was found in significant concentrations in urine of Brazilian and Chinese children and it was positively associated with obesity and DNA damage [Rocha et al., 2018; Han et al., 2021]. TCC exposure during lactation has adverse consequences on the survival of offspring rats [Kennedy et al., 2015]. The evidences against human health led the US Food and Drug Administration (FDA) to prohibit antiseptic wash products containing TCC [Food and Drug Administration, 2016]. However, TCC continues to be incorporated as preservative agent into a number of other personal care products, mainly in other countries, and a large amount of the chemical is released into the sewage and environment exposed to it [Yun et al., 2020; Chen et al., 2019]. It calls attention that TCC has a high potential for bioaccumulation because of resistance to degradation and it is found at high levels in aquatic and terrestrial settings [Yun et al., 2020]. In fact, TCC is one of the most abundant chemical found in wastewater biosolids and, only in China, over 40 tons of this compound are brought to soils each year so that as high as 35 mg/kg of TCC were reported for biosolids retrieved from certain regions of this country [Yun et al., 2020]. In spite of all evidences, many effects of TCC to humans remain controversial and a number of issues surrounding the compound warrant additional research.

The liver is involved in a number of physiological functions, including a pivotal role in body metabolic homeostasis, so that the organ is the almost exclusive site of many pathways linked to intermediary metabolism, such as ureagenesis, ketogenesis and gluconeogenesis [Sharabi et al., 2015; Comar et al., 2010; Oliveira et al., 2014]. The liver is also the most important organ for the biotransformation of drugs and it is exposed to xenobiotics during its metabolic functions [Gu & Manautou, 2012; Eler et al., 2013; Franco-Salla et al., 2019; Pateis et al., 2018]. TCC is metabolized by cytochrome P450 in the liver of rodents and humans and it could affect the hepatic metabolism [Zhang et al., 2020]. In fact, TCC negatively modified the respiration of rat liver isolated mitochondria by a mechanism that involves an oxidative phosphorylation uncoupling action that is similar to those of FCCP, a classic uncoupler agent [Xia et al., 2018]. In addition, metabolomics analysis reveals that the exposure of

cultured hepatocytes to TCC perturbs the oxidative phosphorylation, increases the reactive oxygen species (ROS) production, decreases reduced glutathione (GSH) and ATP content, and creates a prooxidant environment resulting in DNA damage and lipid peroxidation [Zhang et al., 2020]. Metabolomics analysis also reveals that TCC orally administered to mice triggers hepatotoxicity and in addition modifies the hepatic metabolism by mechanisms that probably involve the inhibition of aerobic glycolysis and acceleration of gluconeogenesis, anaerobic glycolysis and  $\beta$ -oxidation of fatty acids [Li et al., 2018]. Gluconeogenesis, however, could not be increased if mitochondrial oxidative phosphorylation is uncoupled and very probable ATP is decreased in the liver. In the same way, gluconeogenesis is extremely sensitive to alterations in cellular integrity because the pathway occurs in different intracellular compartments and requires energy from an aerobic system associated to membranes [Ames-Sibin et al., 2018; Castro-Ghizoni et al., 2017]. Thus, the effects of TCC on gluconeogenesis and other metabolic pathways in the liver remain controversial. Gluconeogenesis and other metabolic pathways in these studies, however, do not rely on flux rate measurements in the liver, but were inferred from metabolomics analysis and gene expression data [Zhang et al., 2020; Li et al., 2018]. However, there is no way of precisely quantifying metabolic pathways from metabolomics analysis or gene expression data, as key enzymes are subjected to highly complex control mechanisms. Therefore, the present study investigated the effects of TCC on gluconeogenesis flux, ureagenesis and glycogen catabolism in perfused livers of rats.

The rat liver in isolated perfusion was used as an experimental tool because it has the great advantage of preserving the organ microcirculation and cell polarity and cell integrity. In addition, TCC can be introduced directly into the portal vein, a situation that would prevent its previous metabolism. This procedure also excludes the long-term effects of TCC, as for example, its actions on gene expression or hepatotoxicity due to chronic exposure. That is, in the present study, only the direct short-term actions of TCC were evaluated in the livers of healthy rats. The actions of TCC on the respiratory activity and the activity of NADH- and succinate oxidases were additionally evaluated in hepatic isolated mitochondria to provide mechanistic insights. The results are hoped to add additional information about the actions TCC with the intact liver cells.

## **2. MATERIALS AND METHODS**

### **2.1. Chemicals**

The rat liver perfusion apparatus was built in the workshops of the State University of Maringá (UEM), Brazil. Standard laboratory diet for rats was purchased from Nuvilab (Colombo, PR, Brazil). Triclocarban – TCC or 1-(4-chlorophenyl)-3-(3,4-dichlorophenyl)urea) – CAS number 101-20-2 and 99% purity, enzymes and coenzymes were purchased from Sigma Chemical Co (St. Louis, MO, USA). All other chemicals were of analytical grade.

### **2.2. Animals**

Male Wistar rats weighting 200-240 g (60 days old) were obtained from the Center of Animal Breeding of the State University of Maringá (UEM) and maintained under standard laboratory conditions at a temperature of  $24 \pm 2^{\circ}\text{C}$  under a regulated 12 hours light/dark cycle. The animals were housed in conventional steel cages (3 rats/cage) and fed *ad libitum* with a standard laboratory diet. After 3 days for acclimatization, animals were used for experiments. For preparing the liver for perfusion or mitochondria isolation the rats were anesthetized by intraperitoneal injection of ketamine (90 mg/kg) and xylazine (9 mg/Kg). The criterion of anesthesia was the lack of body or limb movement in response to a standardized tail clamping stimulus. The procedures followed the guidelines of the Brazilian Council for the Control of Animal Experimentation (CONCEA) and were previously approved by the Ethics Committee for Animal Experimentation (CEUA) of the State University of Maringá (Protocol number CEUA 24391402018).

### **2.3. Liver perfusion and metabolism**

Hemoglobin-free non-recirculating liver perfusion was performed as previously described [Comar et al., 2003]. Deeply anesthetized rats had the peritoneal cavity exposed and, after cannulation of the portal and cava veins, the liver was removed and positioned in a plexiglass chamber. The perfusion fluid was Krebs/Henseleit-bicarbonate buffer (pH 7.4) containing 25 mg% bovine serum albumin and saturated with a mixture of oxygen and carbon dioxide (95:5) by means of a membrane oxygenator with simultaneous

temperature adjustment at 37 °C. The flow was maintained constant by a peristaltic pump (Minipuls 3, Gilson, France). Samples of the effluent perfusion fluid were collected at two minutes intervals and analyzed for their content of metabolites. Gluconeogenesis was measured in livers from 15 h fasted rats. Gluconeogenic substrates used in the perfusion experiments were L-lactate (2 mM), D-fructose (2.5 mM) and L-alanine (2.5 mM), all of which were added to the perfusion fluid. Fed rats possess normal stores of glycogen and were used to investigate glycogen catabolism (glycogenolysis and glycolysis). Due to its low solubility in water, TCC was added to the perfusion fluid, according to the experimental protocols, as a dimethylsulfoxide (DMSO) solution to achieve the final concentration of 5, 10, 25, 50 and 75 µM. DMSO does not significantly affect liver metabolism when infused at rates up to 32 µL/min, which corresponds to a final concentration of 1.4 mM [Acco et al., 2004]. This limit was never surpassed in the present work.

#### **2.4. Metabolite assay**

The samples collected of the effluent perfusion fluid were assayed by means of standard enzymatic procedures: glucose, lactate, pyruvate, ammonia and urea [Bergmeyer, 1974]. Glucose was assayed using the enzymatic-colorimetric glucose oxidase method (505 nm). Lactate and pyruvate were spectrophotometrically quantified (340 nm) using the lactate dehydrogenase reaction with reduction of NAD<sup>+</sup> for lactate assay or oxidation of NADH for pyruvate assay (molar extinction coefficient of  $6.22 \times 10^3 \text{ M}^{-1} \cdot \text{cm}^{-1}$ ) [Bergmeyer, 1974]. Ammonia was assayed by spectrophotometry (340 nm) using the glutamate dehydrogenase method in which the oxidation of NADH was measured [Bergmeyer, 1974]. The subsequent addition of urease allowed to obtain the urea concentration. The oxygen concentration in the venous perfusate was monitored employing a teflon-shielded platinum electrode positioned in a plexiglass chamber at the exit of the perfusate [Sá-Nakanishi et al., 2020]. Metabolic rates were calculated from input-output differences and the total flow rates and expressed as µmol per minute per gram wet liver weight.

#### **2.5. Mitochondria isolation**

Mitochondria were isolated by differential centrifugation as previously

described [Biazon et al., 2016]. Briefly, anesthetized rats had the peritoneal cavity exposed, the liver removed and placed in ice-cold buffer containing 200 mM mannitol, 75 mM sucrose, 0.2 mM ethylene glycol tetraacetic acid (EGTA), 2 mM tris(hydroxymethyl)amino-methane (Tris-HCl), pH 7.4 and 50 mg% bovine serum albumin. The organ was minced, washed and homogenized in the same medium with a Van Potter-Elvehjem homogenizer. The homogenate was then centrifuged sequentially at 600 g (10 min) and 7000 g (10 min). The pellet with the intact mitochondria was washed twice and resuspended with the buffer without EDTA. The protein content in the mitochondrial fraction was measured using the Folin phenol reagent. Hepatic mitochondria were isolated by differential centrifugation [Vilela et al., 2014; Biazon et al., 2016].

## **2.6. Mitochondrial respiration**

Mitochondrial oxygen consumption was measured by polarography using a teflon-shielded platinum electrode [Souza et al., 2021]. Mitochondria were incubated in the closed oxygraph chamber in a medium (2.0 mL) containing 0.25 M mannitol, 5 mM sodium diphosphate, 10 mM KCl, 0.2 mM EDTA and 10 mM Tris-HCl (pH 7.4). Succinate and  $\alpha$ -ketoglutarate, both at a concentration of 10 mM, were used as substrates. TCC was added at various concentrations in the range up to 100  $\mu$ M. Rates of oxygen consumption were computed from the slopes of the recorder tracings and expressed as nmol/(min x mg protein). The respiration rates were measured under three conditions: (a) before the addition of ADP (substrate respiration or basal), (b) just after 0.125 mM ADP addition (state III respiration) and (c) after cessation of the ADP stimulation (state IV). The respiratory control (RC) was calculated as the state III/state IV ratio and the ADP/O ratio was determined as previously described [Sá-Nakanishi et al., 2018].

## **2.7. Mitochondrial membrane-bound oxidases activity**

The activities of NADH-oxidase and succinate-oxidase were measured by polarography using freeze-thawing disrupted mitochondria [Souza et al., 2021]. The incubation medium contained 20 mM Tris-HCl (pH 7,4) and, when appropriate, TCC was added at various concentrations in the range up to 100  $\mu$ M. The reaction was started by the addition of substrates, 1 mM NADH and 1

mM succinate, for NADH-oxidase and succinate-oxidase, respectively. The couple TMPD-ascorbate was in addition used as electron donating substrate to cytochrome c/complex IV of the mitochondrial respiratory chain. Rates of oxygen consumption were computed from the slopes of the recorder tracings and expressed as nmol/(min x mg protein).

## **2.8. Statistical analysis**

The parameters presented in graphs and tables are means  $\pm$  standard errors of the means. Statistical analysis was done by means of the GraphPad Prism Software (version 8.0). The statistical significance of the data was analyzed by means of ANOVA ONE-WAY and the Newman-Keuls post-hoc test was applied with the 5% level of significance ( $p < 0.05$ ). For comparison of two values the student t test was applied with the 5% level ( $p < 0.05$ ). The  $EC_{50}$  and  $IC_{50}$  values were calculated by numerical interpolation with Stineman's formula using the Scientist software from MicroMath Scientific Software (Salt Lake City, UT, USA).

## 3. RESULTS

### 3.1. Effects of TCC on glycogen catabolism and glycolysis

Livers from fed rats when perfused with substrate-free medium survive at the expense of glycogen degradation via glycolysis and oxidation of endogenous fatty acids [Comar et al., 2003]. Under these conditions the liver release glucose, lactate and pyruvate as a result of glycogen catabolism. Fig. 2A illustrates the responses of perfused livers to TCC infusion at the concentration of 75  $\mu\text{M}$ . It also illustrates a typical experimental protocol, which was used for all other TCC concentrations. After a pre-perfusion period of 10 minutes, TCC was infused during 20 minutes, followed by additional 10 minutes of TCC-free perfusion. Four parameters were measured: glucose release, lactate and pyruvate productions and oxygen consumption. As revealed by Fig. 2A all parameters were stable before the initiation of TCC infusion. Upon TCC infusion, oxygen uptake, glucose release and lactate production were stimulated while the pyruvate production was inhibited. After removing the TCC from the perfusion liquid, glucose release, oxygen consumption and lactate production were not substantially modified, but the pyruvate production was increased to values found in the pre-perfusion period.

Experiments like those illustrated in Fig. 2A were repeated with TCC at the concentrations of 5, 10, 25 and 50  $\mu\text{M}$  in order to establish concentration dependences for the effects. For lactate, glucose and oxygen the values represented in Fig. 2B-D are the rates before starting the TCC infusion (8-10 minutes perfusion time; zero TCC concentration) and the rates observed after stabilization of the changes induced by each concentration (26-28 minutes perfusion time). TCC increased by 35%, 82% and 200% the glucose release at the concentrations of 5, 10-50 and 75  $\mu\text{M}$ , respectively, when compared to zero concentration (Fig. 2B). The oxygen uptake was equally stimulated by approximately 24% at TCC concentrations of 25, 50 and 75  $\mu\text{M}$  (Fig. 2C). The lactate production was equally stimulated by 150% from 5  $\mu\text{M}$  and it was maintained elevated until 75  $\mu\text{M}$  (5 - 75  $\mu\text{M}$ ; Fig. 2D). TCC increased by 50% the pyruvate production at the concentration of 25  $\mu\text{M}$  and decreased by 41% at the concentration of 75  $\mu\text{M}$  (Fig. 2E).

The rate of glycogenolysis and glycolysis are represented against the TCC concentration in Fig. 2F and G, respectively. TCC stimulated the glycogenolysis

by 36% at the concentration of 5  $\mu\text{M}$  and equally by 120% at the other higher concentrations (10 – 75  $\mu\text{M}$ ; Fig. 2F). The half-maximal effective concentration ( $\text{EC}_{50}$ ) for stimulation of glycogenolysis can be expected at the portal concentration of 7  $\mu\text{M}$ . TCC stimulated the glycolysis by 44% at the concentration of 5  $\mu\text{M}$  and equally by 135% at the other higher concentrations (10 – 75  $\mu\text{M}$ ; Fig. 2G). The  $\text{EC}_{50}$  for stimulation of glycolysis can be expected at TCC concentration of 6.88  $\mu\text{M}$ . In Fig. 2H, the lactate to pyruvate ratio, an indicator for the cytosolic NADH/NAD<sup>+</sup> ratio [Oliveira et al., 2014], was plotted against the TCC concentration. The infusion of TCC did not modify the NADH/NAD<sup>+</sup> ratio for the concentrations of 5 – 25  $\mu\text{M}$ , but this ratio was increased by 120% at the concentrations of 50 and 75  $\mu\text{M}$ .

### **3.2. Effects of TCC on gluconeogenesis from lactate**

The effect of TCC on gluconeogenesis was investigated in perfused livers using lactate as precursor. The use of L-lactate as the gluconeogenic substrate presents some advantages [Castro-Ghizoni et al., 2017]: it is one of the main gluconeogenic substrates in humans and rodents; it is easily converted into pyruvate by the equilibrium cytosolic enzyme lactate dehydrogenase; and, consequently, allows to evaluate the complete gluconeogenic machinery going through all gluconeogenic steps from pyruvate up to glucose. Fig. 3A shows the time courses of modifications caused by the infusion of 75  $\mu\text{M}$  TCC in perfused livers from rats. It also illustrates a typical experimental protocol, which was used for all other TCC concentrations. Livers from 15 hours fasted rats were perfused in order to ensure low glycogen levels. Under such conditions the rate of glucose output reflects mainly the rate of gluconeogenesis [Comar et al., 2016]. Lactate infusion produced progressive increases in glucose and pyruvate productions and oxygen uptake. These increases tended to stabilize at 34 minutes perfusion time. Upon TCC infusion, the lactate-induced stimulus in the oxygen uptake showed a tendency to increase but it was not modified. TCC infusion initially inhibited the pyruvate production but at the end of its infusion the pyruvate production stimulus was not changed. On the other hand, the lactate-induced stimulus in the glucose production was completely inhibited by 75  $\mu\text{M}$  TCC infusion. After removing the TCC from the perfusion liquid, glucose and after cessation of TCC infusion the pyruvate production was sharply

stimulated and oxygen uptake were not considerably modified.

Experiments like those illustrated in Fig. 3A were repeated with 5, 10, 25 and 50  $\mu\text{M}$  TCC in order to establish concentration dependences for the effects. The values of pyruvate and glucose production and oxygen uptake represented in Fig. 3B, 2C and 2D are the rate before starting the infusion of TCC (32-34 minutes perfusion time; zero TCC concentration) and the rates observed after stabilization of the changes induced by each concentration. The production of pyruvate and the oxygen consumption were not modified by TCC at all concentrations tested. On the other hand, TCC infusion inhibited the glucose production by approximately 50% for the concentrations of 10 and 25  $\mu\text{M}$  and by 80% for the concentrations of 50 and 75  $\mu\text{M}$ . The half-maximal inhibition ( $\text{IC}_{50}$ ) for glucose production can be expected at portal TCC concentration of 17.45  $\mu\text{M}$ .

### **3.3. Effects of TCC on gluconeogenesis and ureagenesis from alanine**

Considering that ureagenesis also requires a considerably energetic apport, this pathway was evaluated in association with gluconeogenesis from alanine. The infusion of alanine permits to evaluate both carbon and nitrogen fluxes in perfused livers. Fig. 4 shows the time courses of modifications on carbon flux (Panel A) and nitrogen flux (Panel B) caused by the infusion of 75  $\mu\text{M}$  TCC on alanine metabolism in perfused livers. It also illustrates a typical experimental protocol, which was used for all other TCC concentrations. Alanine infusion produced progressive increases in glucose, lactate, pyruvate and urea productions. Oxygen uptake and ammonia productions showed a tendency to increase but not statistically significant. These increases tended to stabilize at 32-34 minutes perfusion time. The introduction of 75  $\mu\text{M}$  (at 34 min perfusion time) diminished the glucose production in progressive way, reaching a minimum at 56 min perfusion time. Pyruvate production was decreased and lactate production was increased upon 75  $\mu\text{M}$  TCC infusion. Upon TCC infusion, the alanine-induced stimulus in the oxygen uptake showed a tendency to increase but it was not modified. Urea production was continuously decreased and ammonia production was continuously increased upon TCC infusion. After removing the TCC from the perfusion liquid, lactate and pyruvate productions were reverted but glucose and urea production continued inhibited.

The concentration dependences of the effects of TCC on the carbon and nitrogen fluxes due to alanine infusion are shown in Fig. 5. Glucose production was inhibited by TCC at all concentrations tested (Fig. 5A). The  $IC_{50}$  for glucose production from alanine is expected at TCC concentration of 14.5  $\mu$ M. Oxygen uptake was not modified by TCC, except by a stimulus at the concentration of 50  $\mu$ M (Fig. 5D). The lactate production was increased by 80% and 160%, respectively, for TCC at the concentrations of 50 and 75  $\mu$ M (Fig. 5B). These concentrations of TCC also inhibited considerably the pyruvate production (Fig. 5C). The ammonia production was increased by approximately 120% for TCC at the concentrations of 25, 50 and 75  $\mu$ M (Fig. 5E), but the urea production was inhibited only at the highest concentration of TCC (Fig. 5F).

### 3.4. Effects of TCC on fructose metabolism

In the liver, fructose undergoes both an anabolic energy-dependent conversion into glucose and a catabolic breakdown into lactate and pyruvate (fructolysis; Moreira et al., 2013). Examination of the effects of TCC on fructose metabolism is, thus, an opportunity for evaluating how the compound affects both kinds of metabolism in a single experiment. Fig. 6 shows the results that were obtained in the liver of 15 h fasted rats. Panel A illustrates the time course of the modifications caused by 75  $\mu$ M TCC. Glucose, lactate and pyruvate productions and oxygen consumption were increased when fructose was introduced and all stimulus achieved the steady state 34 min perfusion time. The introduction of TCC at the later time caused a progressive decrease in glucose production. Lactate production and oxygen uptake were slightly increased. Pyruvate production was not modified. The stimulus of the lactate production and oxygen uptake tended to be reversible after ceasing TCC infusion, however, no reversibility of the glucose production was apparent.

Experiments like those illustrated in Fig. 6A were repeated with 5, 10, 25 and 50  $\mu$ M TCC in order to establish concentration dependences for the effects. The values of glucose, pyruvate and glucose production and oxygen uptake represented in Fig. 6B-E are the rate before starting the infusion of TCC (32-34 minutes perfusion time; zero TCC concentration) and the rates observed after stabilization of the changes induced by each concentration (54-56 minutes perfusion time; 5, 10, 25, 50 and 75  $\mu$ M TCC). The lactate/pyruvate ratio are

shown in [Panel F. Fig. 6B](#) shows that glucose production was strongly inhibited by TCC at the concentrations of 25, 50 and 75  $\mu\text{M}$ . The  $\text{IC}_{50}$  for glucose production from fructose can be expected at TCC concentration of 21.4  $\mu\text{M}$ . The production of lactate was increased by TCC only at the concentrations of 10 and 25  $\mu\text{M}$ . Oxygen uptake was slightly increased (approximately 6%) in the presence of all TCC concentrations. The changes in pyruvate production were not statistically significant. The lactate/pyruvate ratio was increased by 28% for TCC at the concentrations of 25, 50 and 75  $\mu\text{M}$ .

### **3.5. Respiration and membrane-bound enzymes activities of isolated mitochondria**

Considering that TCC stimulated the hepatic consumption of oxygen, experiments with isolated mitochondria were done with the purpose of facilitating the interpretation of the data obtained in perfused livers. [Fig. S1](#) outlines the experimental approach used to evaluate the respiratory activity of phosphorylating liver mitochondria and the calculation procedures for obtaining the mitochondrial respiratory parameters. [Fig. 7](#) shows the effects of TCC in the concentration range up to 100  $\mu\text{M}$  on mitochondrial basal respiration, state III respiration and state IV respiration driven by alpha-ketoglutarate ([Panel A](#)) and succinate ([Panel B](#)). Basal respiration was strongly inhibited by TCC added at concentrations equal or higher than 50  $\mu\text{M}$  when alpha-ketoglutarate was the substrate ( $\text{IC}_{50} = 40.4 \mu\text{M}$ ). On the contrary, when succinate was the substrate, basal respiration was stimulated by TCC at concentrations as low as 2.5  $\mu\text{M}$  and had a maximum stimulus at concentrations equal or higher than 10  $\mu\text{M}$  ( $\text{EC}_{50} = 2.39 \mu\text{M}$ ). State III respiration was diminished in a concentration dependent manner irrespective of the substrate (succinate or alpha-ketoglutarate) and a pronounced inhibition was found with TCC at concentrations as low as 2.5 and 5.0  $\mu\text{M}$ . The  $\text{IC}_{50}$  for state III inhibition from alpha-ketoglutarate can be expected at TCC concentration of 5.67  $\mu\text{M}$ . However, state III respiration from succinate was only partially inhibited (50%) even at high concentrations of TCC so that the  $\text{IC}_{50}$  is not calculated for this parameter. State IV respiration was modified exactly in the same manner as the basal respiration, i.e., it was strongly inhibited by TCC when alpha-ketoglutarate was the substrate ( $\text{IC}_{50} = 22.7 \mu\text{M}$ ) and it was stimulated by TCC when succinate was the substrate ( $\text{EC}_{50} = 1.87$

$\mu\text{M}$ ). The respiratory control (RC), which is calculated as state III/state IV, was considerably diminished to values around one by TCC at concentrations as low as 5 and 10  $\mu\text{M}$  irrespective of the substrate (Fig. 8A).

Considering that the state III respiration was inhibited by TCC when both alpha-ketoglutarate and succinate were the substrates, the NADH- and succinate-oxidase activities were further measured in disrupted mitochondria. The results are shown in Fig. 8B. As noted, the activity of both NADH- and succinate oxidase were not modified by TCC, the same way that the oxygen consumption stimulated by the couple TMPD-ascorbate, which is an electron donating substrate to cytochrome c/complex IV of the mitochondrial respiratory chain (Fig. 8B).

## DISCUSSION

TCC was previously reported to perturb the ATP metabolism in isolated hepatocytes and to impair the oxidative phosphorylation of rat liver isolated mitochondria by a mechanism that involves an uncoupling action [Xia et al., 2018; Zhang et al., 2020]. The present study aimed to assess whether these effects occur in the liver under the conditions of a perfused organ, more precisely whether these effects themselves result in modifications of energy-dependent metabolic fluxes in perfused rat livers. In such a structure the tissue organization and cellular integrity are preserved so that TCC achieves the hepatocytes via microcirculation and not by the surrounding medium as that of cell or organelle suspensions. Thus, the amount of TCC that reaches the mitochondria inside the cell, for example, can be limited by other membrane barriers and transformations that occur along the sinusoidal bed. In other words, the amount of TCC reaching the sites at which the effects are exerted may substantially differ from that introduced into the portal bed, which should also occur when the compound achieves the hepatic portal vein after intestinal absorption, for example. Thus, quantitative analysis of the results in addition to the qualitative ones are required to compare properly the effects. In this sense, the half-maximal effective TCC concentration for stimulation ( $EC_{50}$ ) or inhibition ( $IC_{50}$ ) of metabolic fluxes were determined for various parameters.

The results show that TCC modifies several of the energy-dependent metabolic fluxes in the perfused rat livers. In general terms, TCC diminished anabolic processes and increased catabolic fluxes in the organ. These effects were concentration-dependent in their majority. More specifically, TCC inhibited the costly gluconeogenesis from the all three substrates tested, namely lactate, alanine and fructose. TCC also impaired the ammonia detoxification which is also dependent of ATP generated within the mitochondria. The inhibition of gluconeogenesis and ammonia detoxification was accompanied of a stimulus of the liver oxygen consumption, except when the substrate was lactate. The latter seems to be a consequence of a very high oxygen consumption even before of drug infusion, i.e., this parameter seems be already in a maximal stimulus. The combination of both inhibition of these costly pathways associated with stimulus of the oxygen consumption is normally expected from an inhibitor of energy transduction in mitochondria that acts mainly as an uncoupler of oxidative

phosphorylation [Salla et al., 2017]. In relation to catabolic process, glycolysis and fructolysis were stimulated probably as a cytosolic compensatory phenomena for the diminished mitochondrial ATP production. Glycogenolysis was also stimulated probably to provide glucose 6-phosphate for the increased glycolytic flux and biotransformation of TCC. This process was also accompanied by a stimulus of hepatic oxygen consumption, a phenomenon that for 75  $\mu$ M TCC was strongly inhibited by cyanide, an inhibitor of cytochrome c oxidase (mitochondrial electron transport chain), but not additionally modified by the simultaneous infusion of proadifen, an inhibitor of the cytochrome P450 system (endoplasmic reticulum). The latter (data not shown) shows that the stimulus of oxygen consumption was not due to metabolism of TCC by cytochrome P450, but due to an increased activity of the respiratory chain [Eler et al., 2009]. Although the hepatic content of ATP in the presence of TCC has not been determined, the results show that this compound diminishes the efficiency of the mitochondrial energy transduction.

The experiments with isolated hepatic mitochondria represent an attempt at quantitatively determining whether the stimulus of oxygen uptake of perfused livers in the presence of TCC is actually due to an increased activity of the respiratory chain, more precisely due to an uncoupling action. Looking at the increase of basal and state IV respiration stimulated by succinate, TCC seems indeed to act as an uncoupling drug. The same can be said in relation to the loss of mitochondrial respiratory control (RC) caused by TCC in the presence of both succinate and alpha-ketoglutarate. However, inhibition of state III respiration stimulated by both substrates shows that inhibition of electron flow is equally present. For succinate, this effect was found only when the ADP is added (state III respiration), which stimulates the mitochondrial ATP synthesis and it is exactly that occurring during the energetically costly gluconeogenesis [Ames-Sibin et al., 2018]. It is worth stressing that the state III respiration from succinate was only partially inhibited (50%) even at high concentrations of TCC, which can be the consequence of both uncoupling action and inhibition of electron flow simultaneously occurring at the mitochondrial level. This could also be the cause of an only moderate or even absent stimulus of the oxygen consumption associated with a strong and concentration-dependent inhibition of glucose production in perfused livers from the all three substrates tested. In relation to the mechanism by which TCC inhibits the mitochondrial respiration,

it should not be related with the inhibition of electron transport chain at the level of complexes I to IV, i.e., from NADH or succinate until oxygen, the final electron acceptor. This because the inhibition of oxygen uptake was abolished when measured in disrupted mitochondria. One possibility could be the inhibition at the level of the complex ATP synthase. In relation to the complete inhibition of basal, state III and state IV respiration stimulated by alpha-ketoglutarate, it cannot be excluded the possibility of TCC also to inhibit the formation of NADH at the level of alpha-ketoglutarate dehydrogenase enzyme. This because the oxygen consumption was not inhibited by TCC in disrupted mitochondria when NADH is the substrate, but completely inhibited when alpha-ketoglutarate is the substrate in coupled mitochondria, including basal and state IV respiration, which are stimulated by TCC when succinate is the substrate.

The actions of TCC on mitochondrial metabolism should certainly decrease the energetic apport in the form of ATP that is necessary to drive the costly gluconeogenesis. However, the actions on mitochondria are not possibly the only ones responsible for the modifications caused by TCC on the metabolic fluxes in perfused livers. In this regard, the glucose production from lactate, alanine and fructose were inhibited by TCC with an  $IC_{50}$  very similar in the range of 15 to 21  $\mu$ M. Lactate and alanine go through all gluconeogenic steps from pyruvate up to glucose and for this reason need a high energy input in the form of ATP within the mitochondria, more specifically a total apport of six molecules of ATP per molecule of glucose. On the other hand, fructose enters in the gluconeogenesis as glyceraldehyde 3-phosphate plus dihydroxyacetone phosphate and does not pass through the costly initial steps within the mitochondria, although it still requires two molecules of ATP to form the two triose-phosphate molecules in the cytosol [Simões et al., 2017]. In other words, the production of glucose from fructose should be inhibited in a lower extension than that from lactate and alanine if a reduced mitochondrial energetic apport was the only responsible by the TCC actions. Inhibition of regulatory gluconeogenic enzymes that catalyze the final steps of the pathway, namely glucose-6-phosphatase and fructose-1,6-bisphosphatase, should not be excluded. Another possibility could be the hepatic metabolization of TCC, which may not even be the reason for the stimulation of the oxygen consumption in perfused livers, but could divert import amounts of reducing equivalents, which are necessary to cytosolic steps of gluconeogenesis, to produce NADPH

necessary for TCC metabolization. In fact, oxidation of NADPH in consequence of biotransformation reactions has been demonstrated to affect biosynthetic pathways that depend on reducing power in the form of NADPH or NADH, such as gluconeogenesis [Simões et al., 2017; Schloz et al., 1973]. In this regard, the hydroxylation of TTC is the dominant phase I metabolism in hepatic cells [Zhang et al., 2020], a reaction that requires the use of reducing power in the form of NADPH [Simões et al., 2017]. Pronounced oxidative stress in the liver also consumes significant amount of reducing equivalents to neutralize reactive species in the liver [Wendt et al., 2019; Comar et al., 2013] and TCC has been reported to induce elevation of reactive oxygen species (ROS), DNA damage and lipid peroxidation in cultured hepatocytes [Zhang et al., 2020].

In quantitative terms, it can be noted that the concentration range at which TCC impairs the respiratory activity of isolated mitochondria was low and relatively closed with previous study [Xia et al., 2018]. In fact, taking the mitochondrial oxygen consumption stimulation as a measure of uncoupling effect, TCC presented  $EC_{50}$  values around 2  $\mu$ M for succinate-driven basal and state IV respiration and the  $IC_{50}$  for inhibition of alpha-ketoglutarate-driven state III respiration was expected at 5.7  $\mu$ M. On the other hand, the portal concentration range at which TCC modified the metabolic fluxes in perfused livers were relatively higher than those of isolated mitochondria and even isolated cells. The  $IC_{50}$  values for gluconeogenesis from alanine, lactate and fructose were between 14.5 and 21  $\mu$ M. As commented above, this difference can be due at least in part to the preserved tissue organization, particularly, the microcirculation of the perfused organ, in which the amount of portal TCC that reaches the mitochondria inside the cell can be limited by additional membrane barriers and transformations that occur along the sinusoidal bed. On the other hand, glycogenolysis and glycolysis from endogenous glycogen were stimulated at a lower TCC concentration than that found for inhibition of gluconeogenesis. The  $EC_{50}$  expected for glycolysis and glycogenolysis were, respectively, 6.9 and 7.0  $\mu$ M. These values are very similar to that found with other uncouplers like propofol, dinoseb, usnic acid and juglone [Acco et al., 2004; Saling et al., 2011; Moreira et al., 2013; Salla et al., 2017] and represent a cytosolic compensation for an impaired mitochondrial ATP production. In other words, the hepatic metabolism is already affected by TCC in concentrations that still did not inhibit considerably the gluconeogenesis.

The results of the present study show the short-term actions of TCC, i.e., they contribute to understand the acute toxicity features of the compound. When orally administered the drug gains access to the whole organism mainly via the portal vein. TCC produced significant effects on the hepatic energy metabolism at portal concentrations around 5 and 10  $\mu\text{M}$ . There is no information about the portal concentration of TCC after oral ingestion nor after other forms of contamination. However, blood concentrations after oral TCC exposition using personal care products reach values up to 0.5  $\mu\text{M}$  [Schebb et al., 2012], which may be significant for the liver because the portal concentration can be expected to exceed the blood concentration several-fold as previously demonstrated for other drugs [Matsuda et al., 2015]. On the other hand, chronic exposure to TCC may cause medium- and long-term effects, such as alterations on gene expression or hepatotoxicity, as previously demonstrated *in vivo* for mice using metabolomics analysis [Li et al., 2018]. The latter revealed that TCC chronically and orally administered modifies the hepatic metabolism by mechanisms that involves the inhibition of aerobic glycolysis and acceleration of gluconeogenesis. Both phenomena were the opposite to the effects found in the present study, however, they were inferred from metabolomics data and associated with liver damage, a situation that is normally associated with diminution of gluconeogenesis [Ames-Sibin et al., 2018]. For these reasons, the effects found in the present study and others with metabolomics analysis should be complemented with experiments evaluating the actions of TCC orally administered on energy-dependent metabolic fluxes in perfused rat livers.

TCC is a structural analogue of triclosan, which has been commercially used for the same purposes and shares many of actions of TCC on liver metabolism [Pereira-Maróstica et al., 2022]: uncoupling of mitochondrial oxidative phosphorylation, cellular ATP depletion, stimulation of glycolysis and fructolysis, and inhibition of gluconeogenesis and ammonia detoxification. So, it is hard not to quantitatively compare the actions of both compounds in the liver. What calls attention is the concentration range at which triclosan and TCC were active on gluconeogenesis and several other metabolic fluxes [Pereira-Maróstica et al., 2022]. The active portal triclosan concentrations were substantially higher than those expected for TCC. The  $\text{IC}_{50}$  of lactate gluconeogenesis occurred at 73  $\mu\text{M}$  for triclosan and 17.4  $\mu\text{M}$  for TCC, and alanine gluconeogenesis was practically not inhibited by triclosan concentrations up to 50  $\mu\text{M}$  while TCC

considerably inhibited the glucose production from alanine at the concentration of 10  $\mu$ M. The rapid transformation of triclosan in the liver has been reported to reduce its effectiveness as inhibitor of hepatic energy metabolism [Pereira-Maróstica et al., 2022], a phenomenon that may be a probable explanation for the low acute toxicity of triclosan and that could not occur for TCC. In any case, the results show apparently that TCC can present a more acute toxicity, at least on liver metabolism, than its structural analogue triclosan. This evidence should including give more support for regulatory health agencies to prohibit personal care products containing TCC.

## **CONCLUSION**

The study presents the short-term actions of TCC, i.e., the effects that contribute to understand the acute toxicity features of the compound. The results show that TCC produces significant effects on the hepatic energy metabolism at portal concentrations as low as 5  $\mu\text{M}$ . More specifically, TCC inhibited the liver gluconeogenesis from lactate, alanine and fructose and impaired the ammonia detoxification from alanine, which were the consequence mainly of impaired mitochondrial energy metabolism. Glycogenolysis, glycolysis and fructolysis were stimulated probably as a cytosolic compensatory phenomena for the diminished mitochondrial ATP production. The results of isolated mitochondria show that in addition to an uncoupler agent TCC also inhibits the coupled electron flow at the mitochondrial level, which should be the cause of the impaired gluconeogenesis and hepatotoxicity in the liver. These evidences should give more support for regulatory health agencies to prohibit personal care products containing TCC or at least to consider a more deeply evaluation of acute toxicity of the drug.

## **Acknowledgements**

Authors wish to thank the financial support of the Coordenação de Aperfeiçoamento de Pessoal de Nível Superior (CAPES) and of the Conselho Nacional de Desenvolvimento Científico e Tecnológico (CNPq).

## **Competing interests**

The authors declare that no competing interest exists and that all approved the final manuscript.

## REFERENCES

- Acco A, Comar JF, Bracht A. Metabolic effects of propofol in the isolated perfused rat liver. *Basic Clin Pharmacol Toxicol* 2004; 95:166-74. [Doi: 10.1111/j.1742-7843.2004.pto950404.x](https://doi.org/10.1111/j.1742-7843.2004.pto950404.x)
- Ames-Sibin AP, Barizão CL, Castro-Ghizoni CV, Silva FMS, Sá-Nakanishi AB, Bracht L, Bersani-Amado CA, Natali MRM, Bracht A, Comar JF.  $\beta$ -Caryophyllene, the major constituent of copaiba oil, reduces systemic inflammation and oxidative stress in arthritic rats. *J Cell Biochem* 2018;119:10262-10277. [Doi: 10.1002/jcb.27369](https://doi.org/10.1002/jcb.27369)
- Biazon ACB, Wendt MNM, Moreira JR, Ghizoni CVC, Soares AA, Silveira SS, Sá-Nakanishi AB, Amado CAB, Peralta RM, Bracht A, Comar JF. The in vitro antioxidant capacities of hydroalcoholic extracts from roots and leaves of *Smallanthus sonchifolius* (Yacon) do not correlate with their in vivo antioxidant action in diabetic rats. *J. Biosci Med* 4:15-27. [Doi: 10.4236/jbm.2016.42003](https://doi.org/10.4236/jbm.2016.42003)
- Buck Louis GM, Smarr MM, Sun L, Chen Z, Honda M, Wang W, Karthikraj R, Weck J, Kannan K. Endocrine disrupting chemicals in seminal plasma and couple fecundity. *Environ Res* 2018; 163:64-70. [Doi: 10.1016/j.envres.2018.01.028](https://doi.org/10.1016/j.envres.2018.01.028)
- Chen J, Meng XZ, Bergman A, Halden RU. Nationwide reconnaissance of five parabens, triclosan, triclocarban and its transformation products in sewage sludge from China. *J Hazard Mater* 2019; 365:502-510. [Doi: 10.1016/j.jhazmat.2018.11.021](https://doi.org/10.1016/j.jhazmat.2018.11.021)
- Castro-Ghizoni CV, Ames APA, Lameira OA, Bersani-Amado CA, Sá-Nakanishi A. B, Bracht L, Marçal-Natali MR, Peralta RM, Bracht A, Comar JF. Anti-inflammatory and antioxidant actions of copaiba oil are related to liver cell modifications in arthritic rats. *J Cell Biochem* 2017; 118:3409-3423. [Doi: 10.1002/jcb.25998](https://doi.org/10.1002/jcb.25998)
- Comar JF, Suzuki-Kemmelmeier F, Bracht A. The action of oxybutinin on haemodynamics and metabolism in the perfused rat liver. *Basic Clin Pharmacol Toxicol* 2003; 93:147-152. [Doi:10.1034/j.1600-0773.2003.930307.x](https://doi.org/10.1034/j.1600-0773.2003.930307.x)
- Comar JF, Suzuki-Kemmelmeier F, Constantin J, Bracht A. Hepatic zonation of carbon and nitrogen fluxes derived from glutamine and ammonia transformations. *J Biomed Sci* 2010; 17:1. [Doi: 10.1186/1423-0127-17-1](https://doi.org/10.1186/1423-0127-17-1)
- Comar JF, de Oliveira DS, Bracht L, Kemmelmeier FS, Peralta RM, Bracht A. The metabolic responses to L-glutamine of livers from rats with diabetes types 1 and 2. *PLoS One* 2016; 11: e0160067. [Doi: 10.1371/journal.pone.0160067](https://doi.org/10.1371/journal.pone.0160067)
- Comar JF, Babeto de Sá-Nakanishi A, de Oliveira AL, Marques Nogueira Wendt M, Bersani Amado CA, Ishii Iwamoto EL, Peralta RM, Bracht A. Oxidative state of the liver of rats with adjuvant-induced arthritis. *Free Radic Biol Med* 2013; 58:144-153. [Doi: 10.1016/j.freeradbiomed.2012.12.003](https://doi.org/10.1016/j.freeradbiomed.2012.12.003)
- Eler GJ, Peralta RM, Bracht A. The action of n-propyl gallate on gluconeogenesis and oxygen uptake in the rat liver. *Chem Biol Interact* 2009; 181:390-399. [Doi: 10.1016/j.cbi.2009.07.006](https://doi.org/10.1016/j.cbi.2009.07.006)
- Eler GJ, Santos IS, de Moraes AG, Mito MS, Comar JF, Peralta RM, Bracht A. Kinetics of the transformation of n-propyl gallate and structural analogs in the

perfused rat liver. *Toxicol Appl Pharmacol* 2013; 273:35-46. Doi: [10.1016/j.taap.2013.08.026](https://doi.org/10.1016/j.taap.2013.08.026)

Food and Drug Administration, HHS. Safety and Effectiveness of Consumer Antiseptics; Topical Antimicrobial Drug Products for Over-the-Counter Human Use. Final rule. *Fed Regist.* 2016; 81(172):61106-61130. PMID: 27632802

Franco-Salla GB, Bracht L, Parizotto AV, Comar JF, Peralta RM, Bracht F, Bracht A. Kinetics of the metabolic effects, distribution spaces and lipid-bilayer affinities of the organo-chlorinated herbicides 2,4-D and picloram in the liver. *Toxicol Lett* 2019; 313:137-149. Doi: [10.1016/j.toxlet.2019.06.008](https://doi.org/10.1016/j.toxlet.2019.06.008)

Gu X, Manautou JE. Molecular mechanisms underlying chemical liver injury. *Expert Rev Mol Med.* 2012 14:e4. Doi: [10.1017/S1462399411002110](https://doi.org/10.1017/S1462399411002110)

Halden RU, Lindeman AE, Aiello AE, Andrews D, Arnold WA, Fair P, Fuoco RE, Geer LA, Johnson PI, Lohmann R, McNeill K, Sacks VP, Schettler T, Weber R, Zoeller RT, Blum A. The florence statement on triclosan and triclocarban. *Environ Health Perspect* 2017; 125:064501. Doi: [10.1289/EHP1788](https://doi.org/10.1289/EHP1788)

Han M, Wang Y, Tang C, Fang H, Yang D, Wu J, Wang H, Chen Y, Jiang Q. Association of triclosan and triclocarban in urine with obesity risk in Chinese school children. *Environ Int* 2021; 157:106846. Doi: [10.1016/j.envint.2021.106846](https://doi.org/10.1016/j.envint.2021.106846)

Hernández-Moreno D, Blázquez M, Andreu-Sánchez O, Bermejo-Nogales A, Fernández-Cruz ML. Acute hazard of biocides for the aquatic environmental compartment from a life-cycle perspective. *Sci Total Environ* 2019; 658:416-423. Doi: [10.1016/j.scitotenv.2018.12.186](https://doi.org/10.1016/j.scitotenv.2018.12.186)

Iacopetta D, Catalano A, Ceramella J, Saturnino C, Salvagno L, Ielo I, Drommi D, Scali E, Plutino MR, Rosace G, Sinicropi MS. The different facets of triclocarban: a review. *Molecules* 2021; 26:2811. Doi: [10.3390/molecules26092811](https://doi.org/10.3390/molecules26092811)

Kennedy RC, Menn FM, Healy L, Fecteau KA, Hu P, Bae J, Gee NA, Lasley BL, Zhao L, Chen J. Early life triclocarban exposure during lactation affects neonate rat survival. *Reprod Sci* 2015; 22:75-89. Doi: [10.1177/1933719114532844](https://doi.org/10.1177/1933719114532844)

Kim SA, Rhee MS. Microbicidal effects of plain soap vs triclocarban-based antibacterial soap. *J Hosp Infect* 2016; 94:276-280. Doi: [10.1016/j.jhin.2016.07.010](https://doi.org/10.1016/j.jhin.2016.07.010)

Li W, Zhang W, Chang M, Ren J, Xie W, Chen H, Zhang Z, Zhuang X, Shen G, Li H. Metabonomics reveals that triclocarban affects liver metabolism by affecting glucose metabolism,  $\beta$ -oxidation of fatty acids, and the TCA cycle in male mice. *Toxicol Lett* 2018; 299:76-85. Doi: [10.1016/j.toxlet.2018.09.011](https://doi.org/10.1016/j.toxlet.2018.09.011)

Lima LC, GD Buss, EL Ishii-Iwamoto, CL Salgueiro-Pagadigorria, JF Comar, A Bracht, J Constantin, Metabolic effects of p-coumaric acid in the perfused rat liver. *J Biochem Mol Toxicol* 2006; 20:18-26. Doi: [10.1002/jbt.20114](https://doi.org/10.1002/jbt.20114)

Maillard JY. Resistance of bacteria to biocides. *Microbiol Spectr* 2018; 6, ARBA-0006-2017. Doi: [10.1128/microbiolspec.ARBA-0006-2017](https://doi.org/10.1128/microbiolspec.ARBA-0006-2017)

Moreira CT, Oliveira AL, Comar JF, Peralta RM, Bracht A. Harmful effects of usnic acid on hepatic metabolism. *Chem Biol Interact* 2013; 203:502-511. [Doi: 10.1016/j.cbi.2013.02.001](https://doi.org/10.1016/j.cbi.2013.02.001)

Oliveira AL, Comar JF, de Sá-Nakanishi AB, Peralta RM, Bracht A. The action of p-synephrine on hepatic carbohydrate metabolism and respiration occurs via both Ca(2+)-mobilization and cAMP production. *Mol Cell Biochem* 2014; 388:135-147. [Doi: 10.1007/s11010-013-1905-2](https://doi.org/10.1007/s11010-013-1905-2)

Pateis VO, Bracht L, Castro LS, Franco-Salla GB, Comar JF, Parizotto AV, Peralta RM, Bracht A. The food additive BHA modifies energy metabolism in the perfused rat liver. *Toxicol Lett* 2018; 299:191-200. [Doi: 10.1016/j.toxlet.2018.10.005](https://doi.org/10.1016/j.toxlet.2018.10.005)

Pereira-Maróstica HV, Bracht L, Comar JF, Peralta RM, Bracht A, Sá-Nakanishi AB. The rapid transformation of triclosan in the liver reduces its effectiveness as inhibitor of hepatic energy metabolism. *Toxicol Appl Pharmacol* 2022; 442:115987. [Doi: 10.1016/j.taap.2022.115987](https://doi.org/10.1016/j.taap.2022.115987)

Petersen S, Mack C, de Graaf AA, Ridet C, Eikmanns BJ, Sahm H. Metabolic consequences of altered phosphoenolpyruvate carboxylase activity in *Corynebacterium glutamicum* reveal anaplerotic regulation mechanism in vivo. *Metab Eng* 2001; 3:344-361. [DOI: 10.1006/mben.2001.0198](https://doi.org/10.1006/mben.2001.0198)

Rocha BA, Asimakopoulos AG, Honda M, da Costa NL, Barbosa RM, Barbosa F Jr, Kannan K. Advanced data mining approaches in the assessment of urinary concentrations of bisphenols, chlorophenols, parabens and benzophenones in Brazilian children and their association to DNA damage. *Environ Int* 2018; 116:269-277. [Doi: 10.1016/j.envint.2018.04.023](https://doi.org/10.1016/j.envint.2018.04.023)

Sá-Nakanishi AB, Soni-Neto J, Moreira LS, Gonçalves GA, Silva-Comar FMS, Bracht L, Bersani-Amado CA, Peralta RM, Bracht A, Comar JF. Anti-inflammatory and antioxidant actions of methyl jasmonate are associated with metabolic modifications in the liver of arthritic rats. *Oxid Med Cell Longev* 2018; 2018:2056250. [DOI: 10.1155/2018/2056250](https://doi.org/10.1155/2018/2056250)

Sá-Nakanishi AB, de Oliveira MC, O Pateis V, P Silva LA, Pereira-Maróstica HV, Gonçalves GA, S Oliveira MA, Godinho J, Bracht L, Milani H, Bracht A, Comar JF. Glycemic homeostasis and hepatic metabolism are modified in rats with global cerebral ischemia. *Biochim Biophys Acta Mol Basis Dis* 2020, 1866:165934. [Doi: 10.1016/j.bbadis.2020.165934](https://doi.org/10.1016/j.bbadis.2020.165934)

Saling SC, Comar JF, Mito MS, Peralta RM, Bracht A. Actions of juglone on energy metabolism in the rat liver. *Toxicol Appl Pharmacol* 2011; 257:319-27. [Doi: 10.1016/j.taap.2011.09.004](https://doi.org/10.1016/j.taap.2011.09.004)

Sharabi K, Tavares CDJ, Rines AK, Puigserver P. Molecular pathophysiology of hepatic glucose production. *Mol Aspects Med* 2015; 46:21-33. [Doi: 10.1016/j.mam.2015.09.003](https://doi.org/10.1016/j.mam.2015.09.003)

Schebb NH, Inceoglu B, Ahn KC, Morisseau C, Gee SJ, Hammock BD. Investigation of human exposure to triclocarban after showering and preliminary evaluation of its biological effects. *Environ Sci Technol* 2011; 45:3109-3115. [Doi: 10.1021/es103650m](https://doi.org/10.1021/es103650m)

Schebb NH, Ahn KC, Dong H, Gee SJ, Hammock BD. Whole blood is the sample matrix of choice for monitoring systemic triclocarban levels. *Chemosphere* 2012;87:825-827. Doi: [10.1016/j.chemosphere.2011.12.077](https://doi.org/10.1016/j.chemosphere.2011.12.077)

Scholz R, Hansen W, Thurman RG. Interaction of mixed-function oxidation with biosynthetic processes. 1. Inhibition of gluconeogenesis by aminopyrine in perfused rat liver. *Eur J Biochem* 1973; 38:64-72. Doi: [10.1111/j.1432-1033.1973.tb03034.x](https://doi.org/10.1111/j.1432-1033.1973.tb03034.x)

Simões MS, Bracht L, Parizotto AV, Comar JF, Peralta RM, Bracht A. The metabolic effects of diuron in the rat liver. *Environ Toxicol Pharmacol* 2017; 54:53-61. Doi: [10.1016/j.etap.2017.06.024](https://doi.org/10.1016/j.etap.2017.06.024)

Souza KS, Moreira LS, Silva BT, Oliveira BPM, Carvalho AS, Silva PS, Verri WA Jr, Sá-Nakanishi AB, Bracht L, Zanoni JN, Gonçalves OH, Bracht A, Comar JF. Low dose of quercetin-loaded pectin/casein microparticles reduces the oxidative stress in arthritic rats. *Life Sci* 2021; 284:119910. Doi: [10.1016/j.lfs.2021.119910](https://doi.org/10.1016/j.lfs.2021.119910)

Vilela VR, Oliveira AL, Comar JF, Peralta RM, Bracht A. Effects of tadalafil on the cAMP stimulated glucose output in the rat liver. *Chem Biol Interact* 2014; 220: 1-11. Doi: [10.1016/j.cbi.2014.05.020](https://doi.org/10.1016/j.cbi.2014.05.020)

Wei L, Qiao P, Shi Y, Ruan Y, Yin J, Wu Q, Shao B. Triclosan/triclocarban levels in maternal and umbilical blood samples and their association with fetal malformation. *Clin Chim Acta* 2017; 466:133-137. Doi: [10.1016/j.cca.2016.12.024](https://doi.org/10.1016/j.cca.2016.12.024)

Wendt MNM, de Oliveira MC, Castro LS, Franco-Salla GB, Parizotto AV, Silva FMS, Natali MRM, Bersani-Amado CA, Bracht A, Comar JF. Fatty acids uptake and oxidation are increased in the liver of rats with adjuvant-induced arthritis. *Biochim Biophys Acta (BBA) Mol Basis Dis* 2019; 1865:696-707. Doi: [10.1016/j.bbadis.2018.12.019](https://doi.org/10.1016/j.bbadis.2018.12.019)

Xia M, Huang R, Shi Q, Boyd WA, Zhao J, Sun N, Rice JR, Dunlap PE, Hackstadt AJ, Bridge MF, Smith MV, Dai S, Zheng W, Chu PH, Gerhold D, Witt KL, DeVito M, Freedman JH, Austin CP, Houck KA, Thomas RS, Paules RS, Tice RR, Simeonov A. Comprehensive analyses and prioritization of Tox21 10K chemicals affecting mitochondrial function by in-depth mechanistic studies. *Environ Health Perspect* 2018; 126:077010. Doi: [10.1289/EHP2589](https://doi.org/10.1289/EHP2589)

Xie M, Zhang H, Wang W, Sherman HL, Minter LM, Cai Z, Zhang G. Triclocarban exposure exaggerates spontaneous colonic inflammation in Il-10<sup>-/-</sup> mice. *Toxicol Sci* 2020; 174:92-99. Doi: [10.1093/toxsci/kfz248](https://doi.org/10.1093/toxsci/kfz248)

Yin J, Wei L, Shi Y, Zhang J, Wu Q, Shao B. Chinese population exposure to triclosan and triclocarban as measured via human urine and nails. *Environ Geochem Health* 2016; 38:1125-1135. Doi: [10.1007/s10653-015-9777-x](https://doi.org/10.1007/s10653-015-9777-x)

Yun H, Liang B, Kong D, Li X, Wang A. Fate, risk and removal of triclocarban: A critical review. *J Hazard Mater* 2020; 387:121944. Doi: [10.1016/j.jhazmat.2019.121944](https://doi.org/10.1016/j.jhazmat.2019.121944)

Zhang H, Lu Y, Liang Y, Jiang L, Cai Z. Triclocarban-induced responses of endogenous and xenobiotic metabolism in human hepatic cells: Toxicity

assessment based on nontargeted metabolomics approach. J Hazard Mater  
2020; 392:122475. Doi: [10.1016/j.jhazmat.2020.122475](https://doi.org/10.1016/j.jhazmat.2020.122475)

## FIGURE CAPTIONS

**Fig. 1.** *Planar structure of triclocarban (TCC).*

**Fig. 2.** *Effects of TCC on glycogen catabolism in the perfused livers of rats.*

**Panel A:** time courses of glucose release, lactate and pyruvate productions and oxygen consumption in the livers from fed rats perfused with TCC at the concentration of 75  $\mu\text{M}$ , as indicated by the horizontal bar in Panel A. The outflowing perfusate was sampled in regular intervals and analyzed for their contents of metabolites. Oxygen uptake was monitored by polarography. Data are the mean  $\pm$  SEM obtained from 4 animals. TCC was infused also at the concentrations of 5, 10, 25 and 50  $\mu\text{M}$  according to the same protocol illustrated in Panel A. The values in **Panels B, C, D and E** are the rates before starting the TCC infusion (8-10 minutes perfusion time; zero TCC concentration) and the rates observed after stabilization of the changes induced by each concentration. The values in **Panels F and G** were calculated from the steady-state rates of glucose, lactate and pyruvate production. Glycogenolysis = glucose +  $1/2(\text{lactate} + \text{pyruvate})$  and glycolysis =  $1/2(\text{lactate} + \text{pyruvate})$ . Each datum represents the mean of 4 liver perfusion experiments. Values with different superscript letters are statistically different ( $p < 0.05$ ; ANOVA ONE-WAY and the Newman-Keuls post-hoc).

**Fig. 3.** *The concentration-dependent effects of TCC on gluconeogenesis from lactate in the perfused livers of rats.*

**Panel A:** time courses of glucose and pyruvate production and oxygen consumption due to lactate infusion. Livers from 15 h fasted rats were perfused with 2 mM L-lactate and TCC as indicated by the horizontal bar in Panel A. The outflowing perfusate was sampled in regular intervals and analyzed for their contents of glucose and pyruvate. Oxygen uptake was monitored by polarography. The values in **Panels B, C and D** are the rate before starting the infusion of TCC (32-34 minutes perfusion time in Fig. 3A; zero TCC concentration) and the rates observed after stabilization of the changes induced by TCC (54-56 min perfusion time in Panel A). Data are the mean  $\pm$  SEM obtained from 4 animals for each condition. Values with different superscript letters are statistically different ( $p < 0.05$ ; ANOVA ONE-WAY and the Newman-Keuls post-hoc).

**Fig. 4.** *Time courses of the effects of TCC on gluconeogenesis and ureagenesis from alanine in the perfused livers of rats.* **Panel A:** time courses of glucose, lactate and pyruvate production due to L-alanine infusion. **Panel B:** time courses of ammonia and urea production and oxygen consumption due to L-alanine infusion. Livers from 15 h fasted rats were perfused with 2.5 mM L-alanine and 75  $\mu$ M TCC as indicated by the horizontal bars. The outflowing perfusate was sampled in regular intervals and analyzed for their contents of glucose, lactate, pyruvate, urea and ammonia. Oxygen uptake was monitored by polarography. Data are the mean  $\pm$  SEM obtained from 4 animals for each condition.

**Fig. 5.** *The concentration-dependent effects of TCC on gluconeogenesis from and ureagenesis from alanine in the perfused livers of rats.* Livers from 15 h fasted rats were perfused with 2.5 mM L-alanine and TCC (10, 25, 50 and 75  $\mu$ M) as indicated by the horizontal bar in [Fig. 4A and B](#). The outflowing perfusate was sampled in regular intervals and analyzed for their contents of glucose, lactate, pyruvate, urea and ammonia. glucose and pyruvate. Oxygen uptake was monitored by polarography. The values in **Panels A - F** are the rate before starting the infusion of TCC (32-34 minutes perfusion time in [Fig. 4A and B](#); zero TCC concentration) and the rates observed after stabilization of the changes induced by TCC (54-56 min perfusion time in [Fig. 4A and B](#)). Data are the mean  $\pm$  SEM obtained from 4 animals for each condition. Values with different superscript letters are statistically different ( $p < 0.05$ ; ANOVA ONE-WAY and the Newman-Keuls post-hoc).

**Fig. 6.** *The concentration-dependent effects of TCC on gluconeogenesis and glycolysis from D-fructose in the perfused livers of rats.* **Panel A:** time courses of glucose, lactate and pyruvate production and oxygen consumption due to fructose infusion. Livers from 15 h fasted rats were perfused with 2.5 mM D-fructose and TCC as indicated by the horizontal bar in Panel A. The outflowing perfusate was sampled in regular intervals and analyzed for their contents of glucose, lactate and pyruvate. Oxygen uptake was monitored by polarography. The values in **Panels B, C, D, E and F** are the rate before starting the infusion of TCC (32-34 minutes perfusion time in [Fig. 6A](#); zero TCC concentration) and the rates observed after stabilization of the changes induced by TCC (54-56 min

perfusion time in Panel A). Data are the mean  $\pm$  SEM obtained from 4 animals for each condition. Values with different superscript letters are statistically different ( $p < 0.05$ ; ANOVA ONE-WAY and Newman-Keuls post-hoc).

**Fig. 7.** *The concentration-dependent effects of TCC on the respiratory activity of isolated hepatic mitochondria.* Isolated coupled mitochondria ( $1.0 \text{ mg}\cdot\text{mL}^{-1}$ ) were incubated at  $37^\circ\text{C}$  in a closed oxygraph chamber containing 2 mL of the reaction medium and TCC at the concentration range up to  $100 \text{ }\mu\text{M}$ . The experimental protocol and calculation procedures are shown in Fig. S1. Mitochondrial respiration driven by alpha-ketoglutarate (**Panel A**) or succinate (**Panel B**) before the addition of ADP (basal), just after  $0.125 \text{ mM}$  ADP addition (state III respiration) and after cessation of the ADP stimulation (state IV) was followed polarographically. Data represent the mean  $\pm$  SEM of 5 animals. \* $p < 0.05$ : different from  $0.0 \text{ }\mu\text{M}$  TCC (ANOVA ONE-WAY and the Newman-Keuls post-hoc).

**Fig. 8.** *The concentration-dependent effects of TCC on the respiratory control of coupled mitochondria and the oxidases activity of disrupted mitochondria.* **Panel A:** respiratory control calculated as state III/state IV from data obtained of phosphorylating intact mitochondria in Fig. 7. **Panel B:** membrane-bound NADH oxidase and succinate oxidase activities and oxygen consumption from TMPD/ascorbate measured in disrupted mitochondria. Data represent the mean  $\pm$  SEM of 4 animals. \* $p < 0.05$ : different from  $0.0 \text{ }\mu\text{M}$  TCC (ANOVA ONE-WAY and the Newman-Keuls post-hoc).

**Fig. S1.** Oxygraph (A) and experimental approach used to determine the respiratory activity of isolated mitochondria (B).

**Fig. 2**

**A:** Time courses of glycogen catabolism

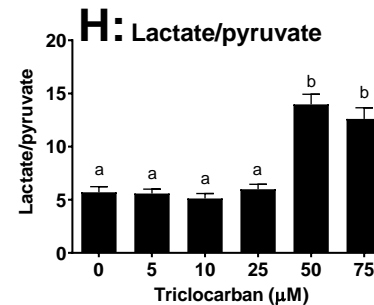
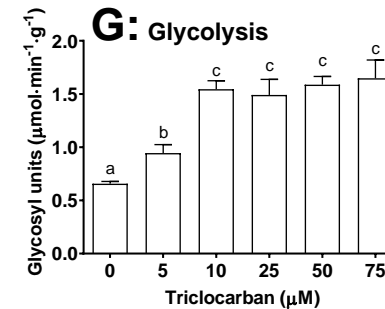
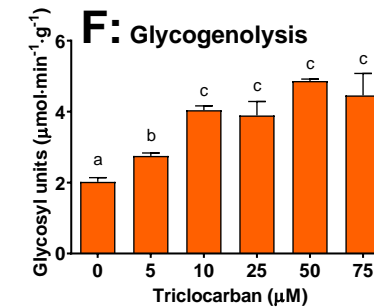
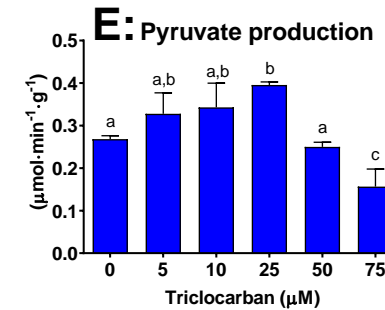
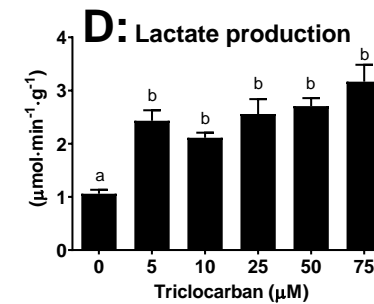
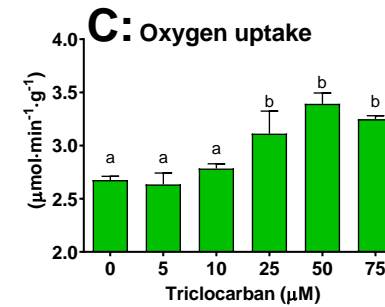
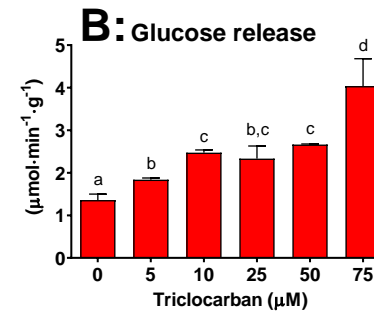
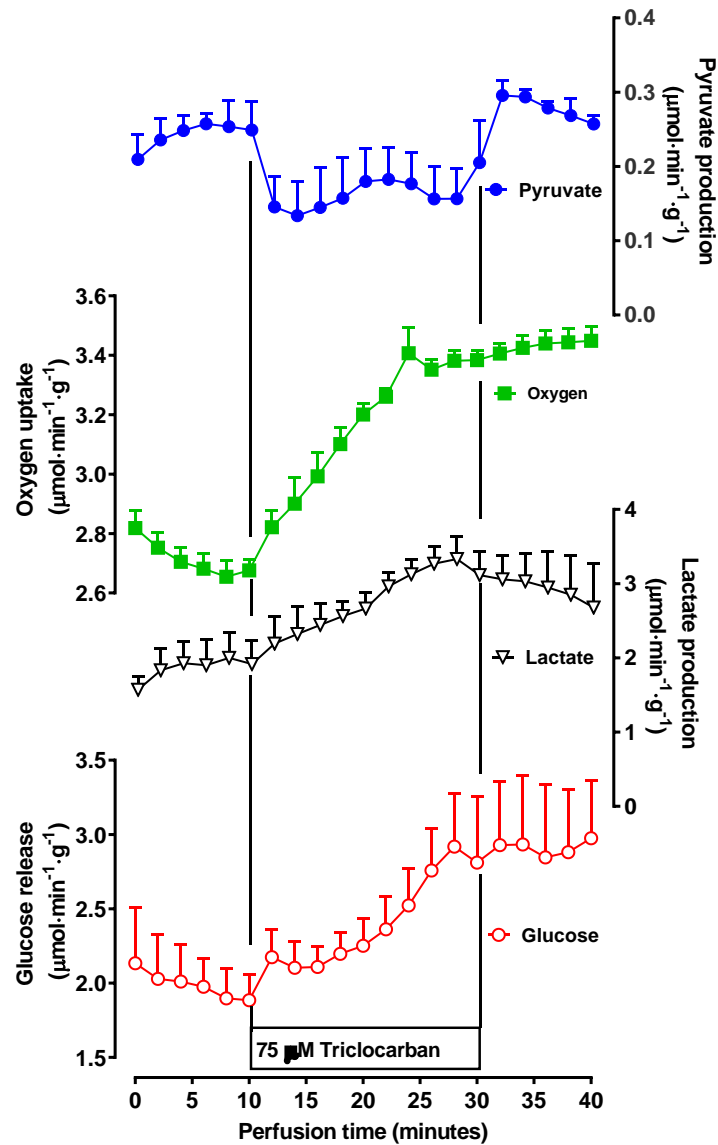


**Fig. 3**

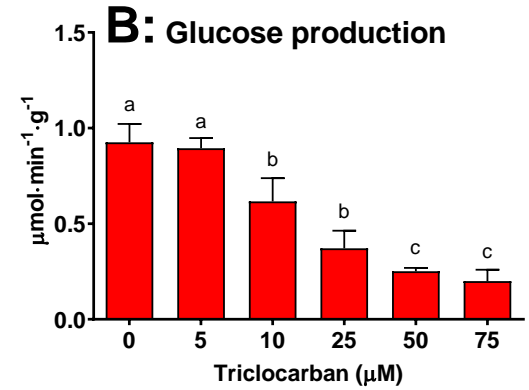
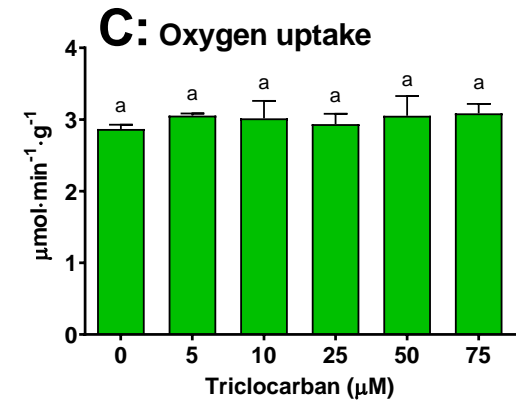
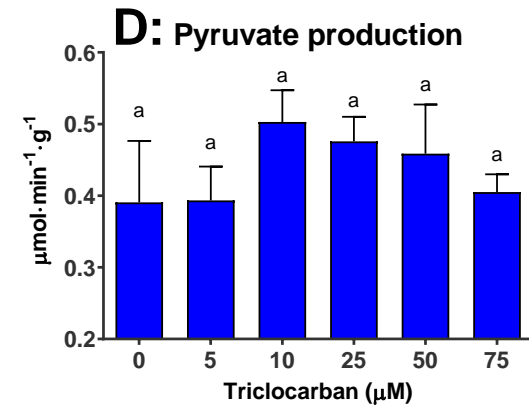
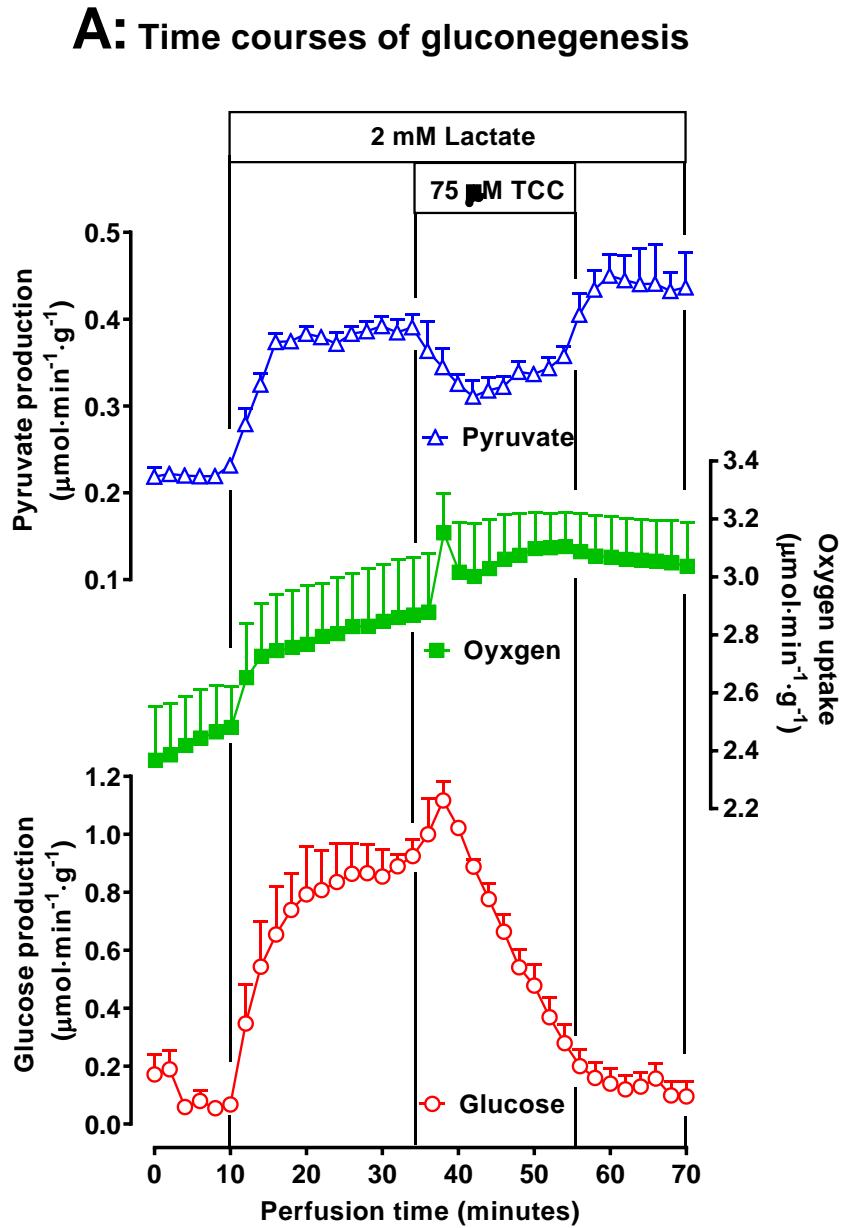
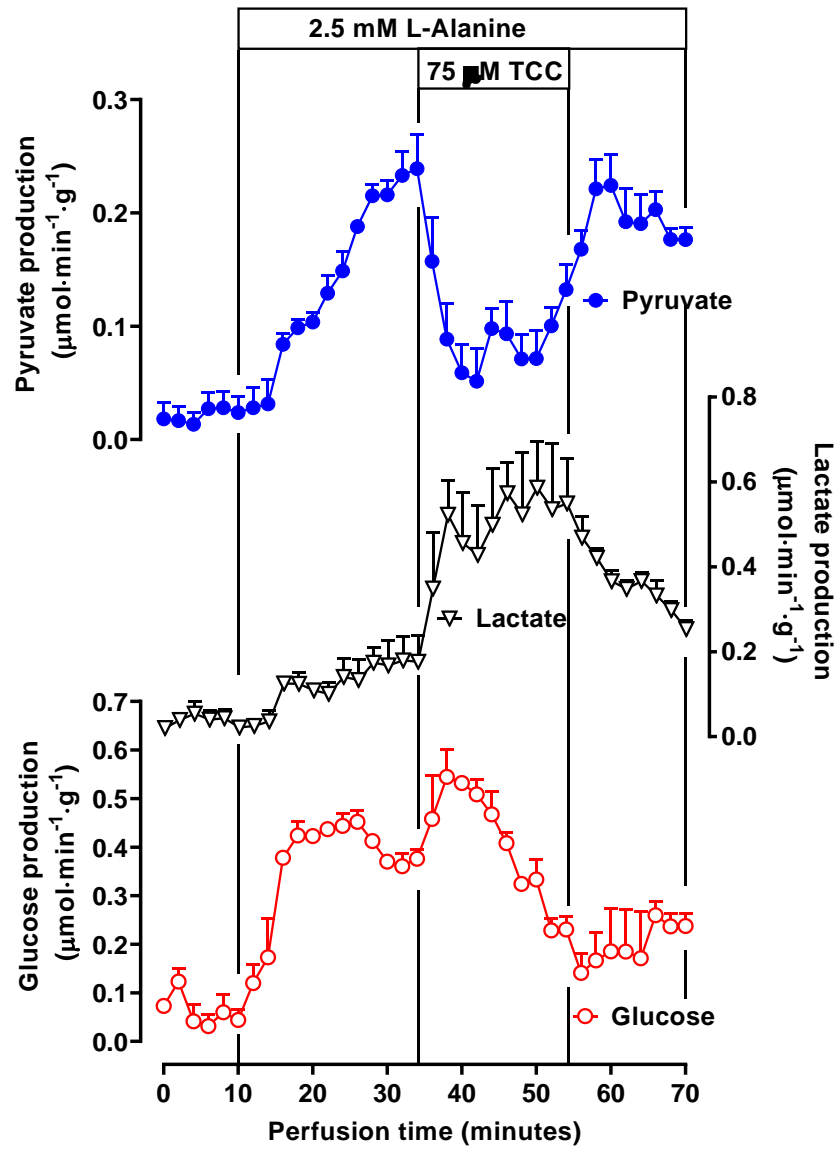
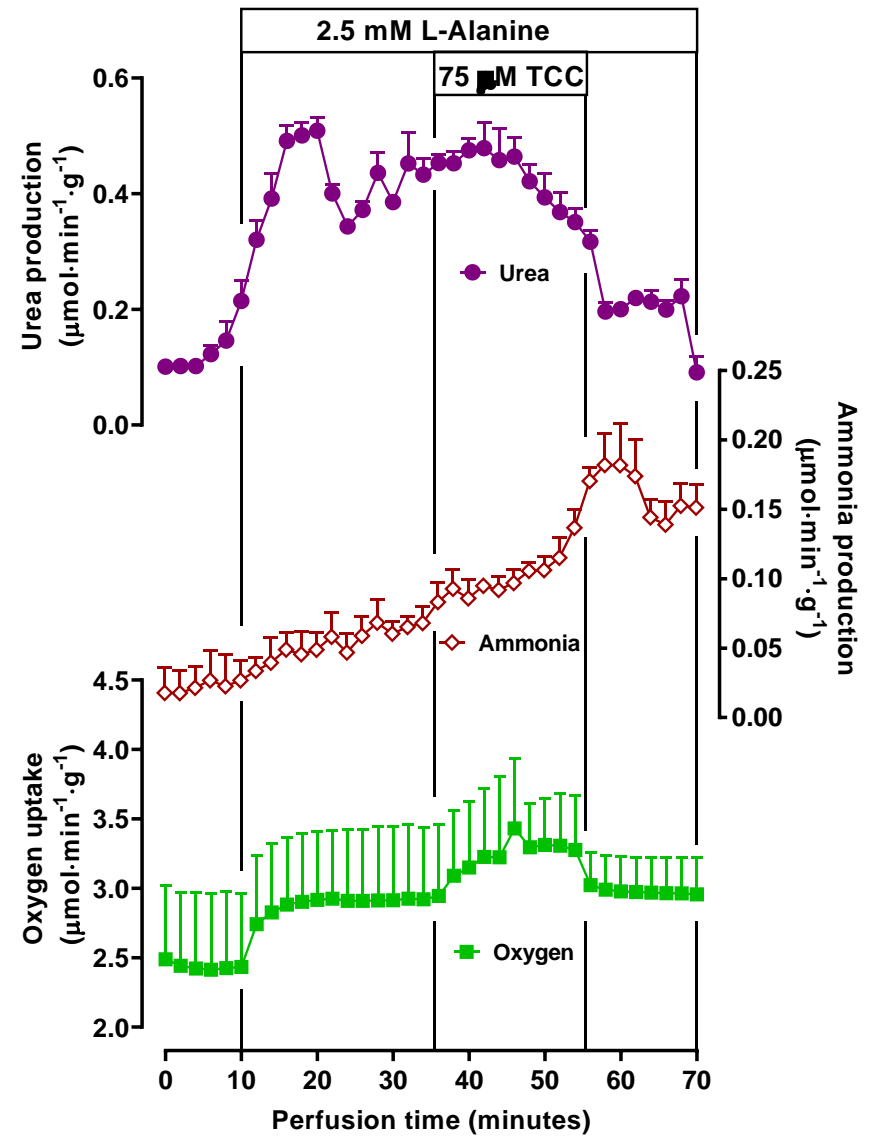


Fig. 4

**A:** Time courses of gluconeogenesis



**B:** Time courses of ureagenesis



**Fig. 5**

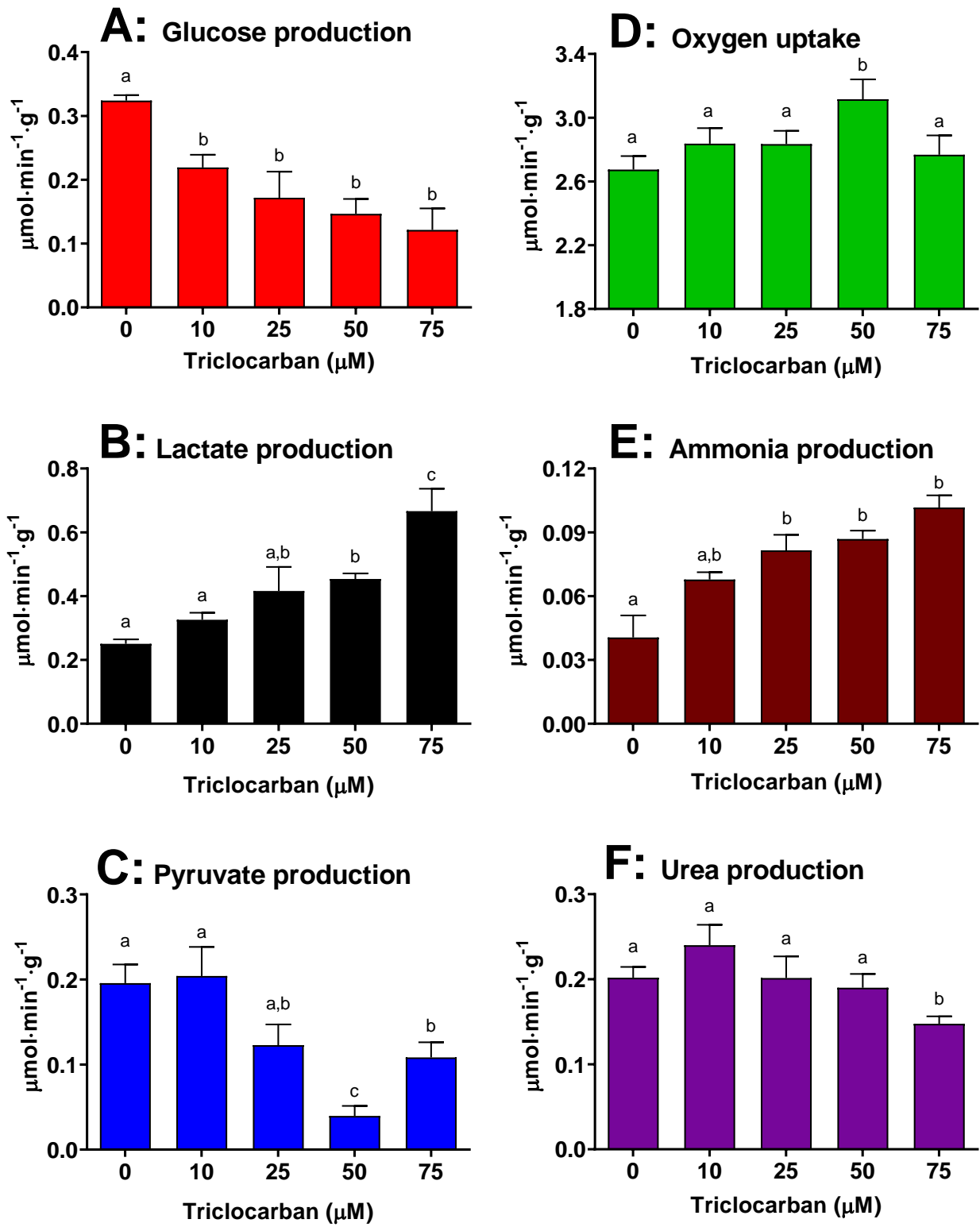
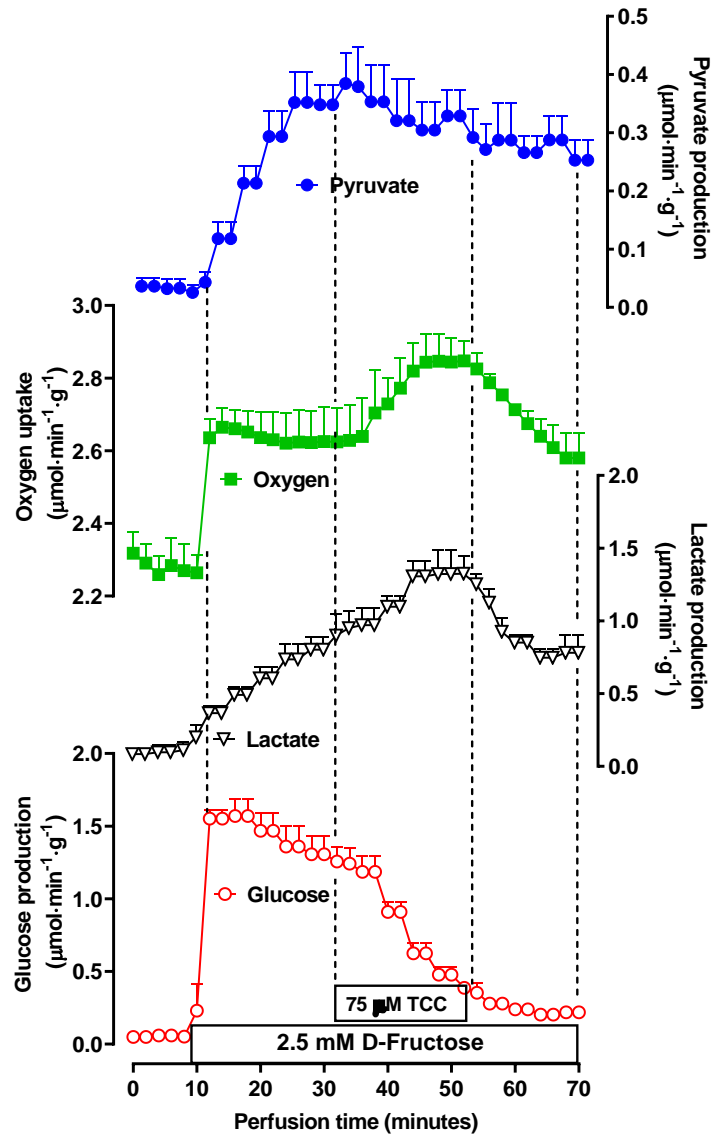
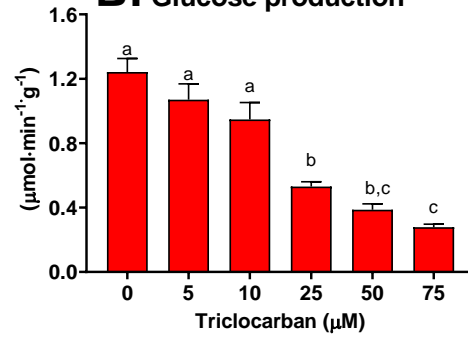


**Fig. 6**

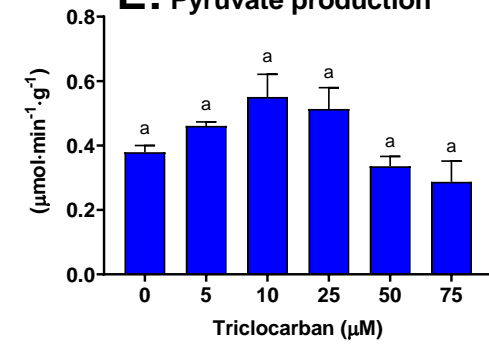
**A: Fructose metabolism**



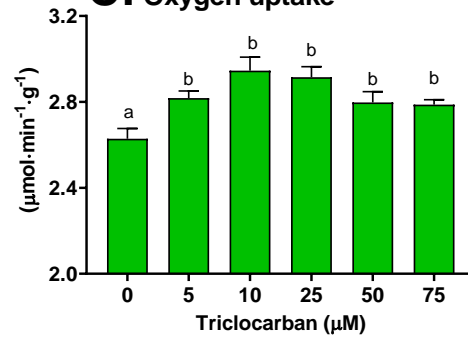
**B: Glucose production**



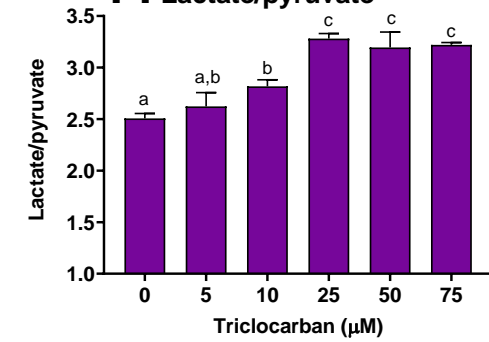
**E: Pyruvate production**



**C: Oxygen uptake**



**F: Lactate/pyruvate**



**D: Lactate production**

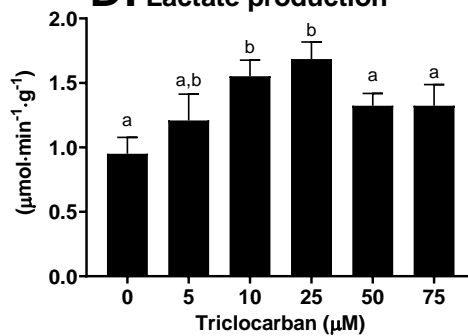


Fig. 7

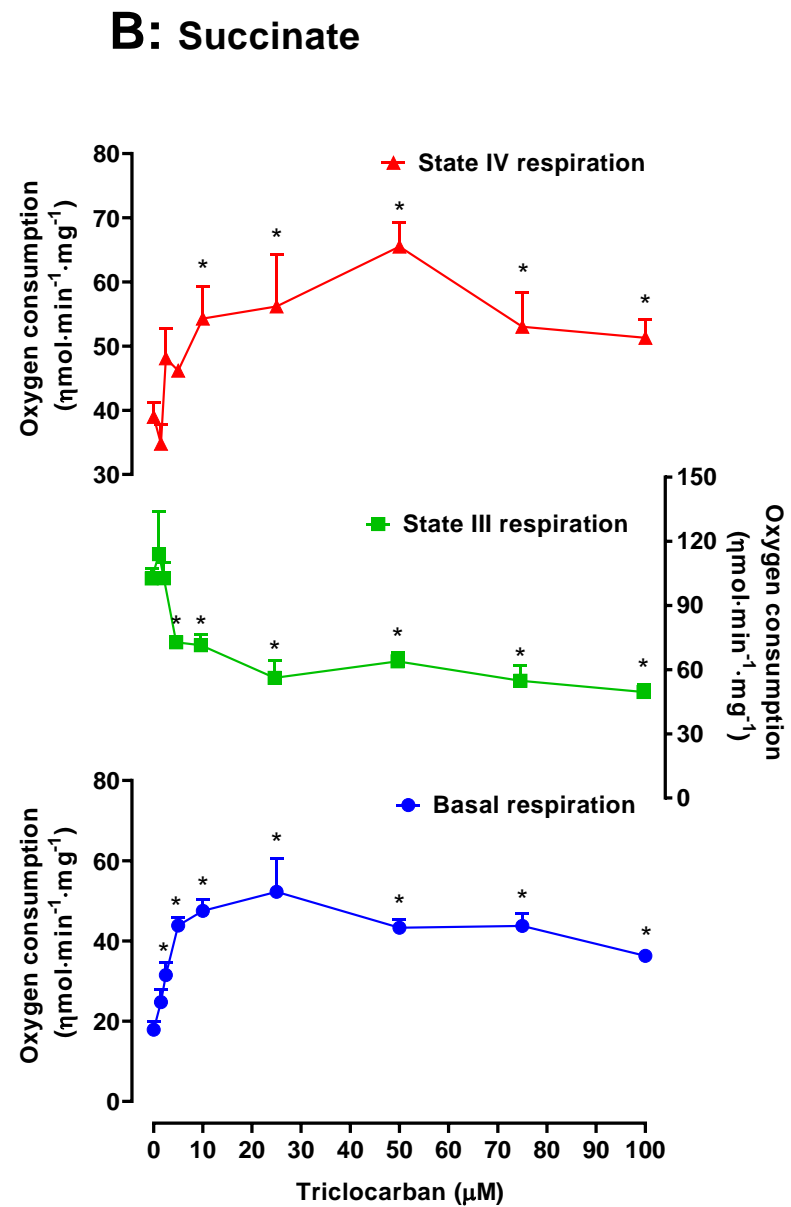
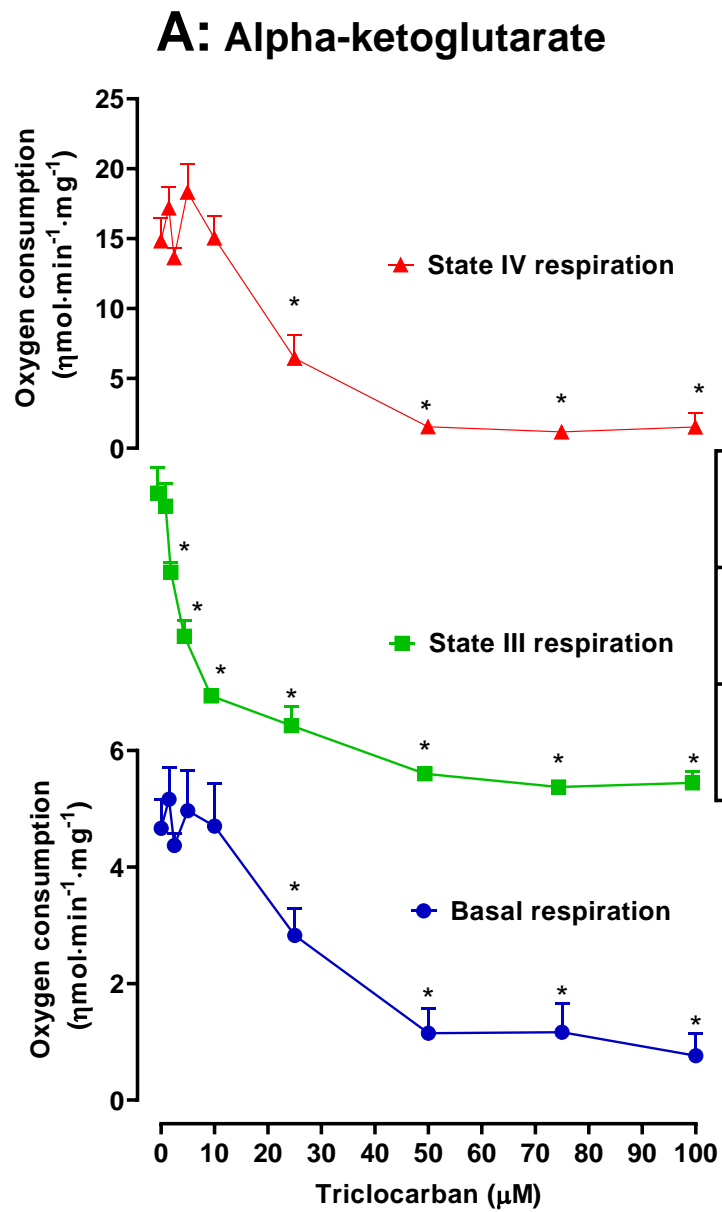
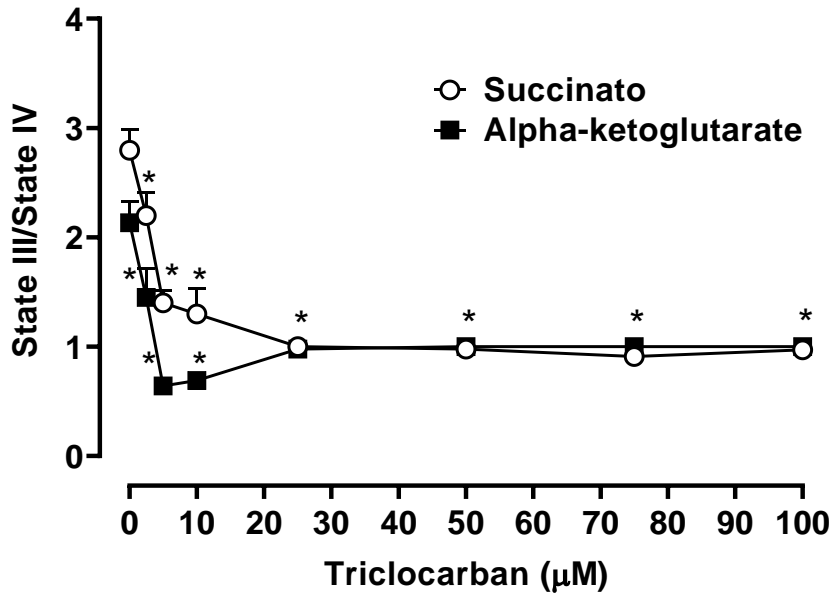
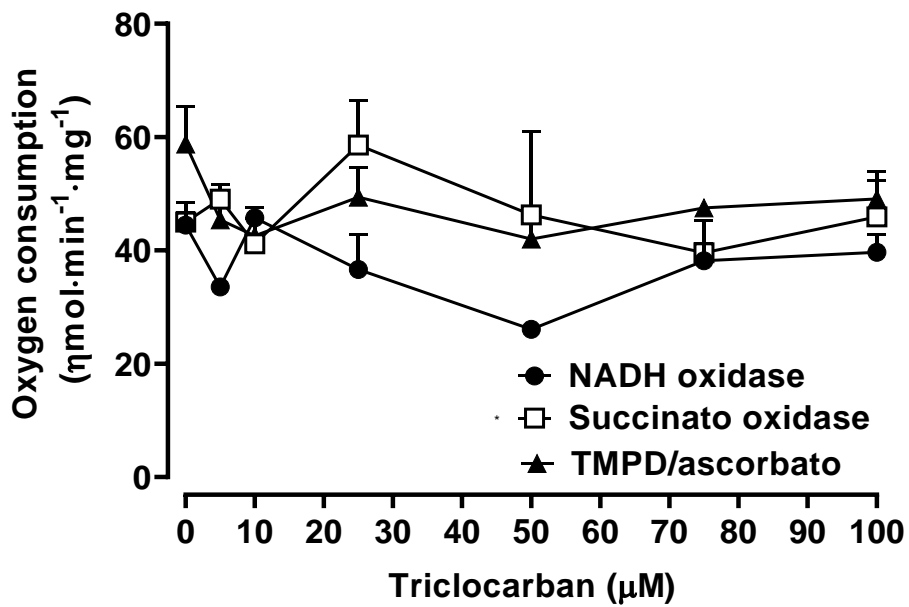


Fig. 8

## A: Respiratory control (RC)



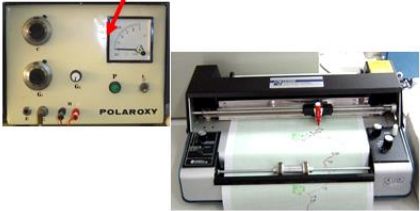
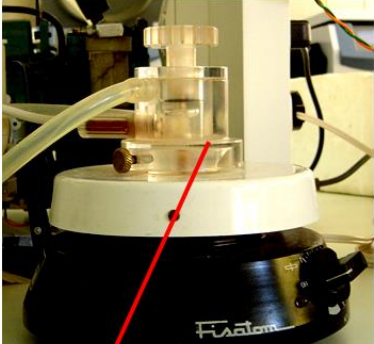
## B: Mitochondrial oxidases activity



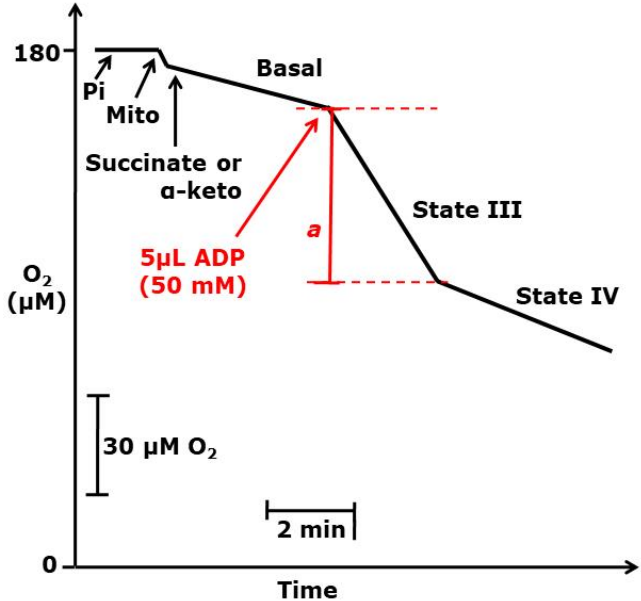
# SUPPLEMENTARY MATHERIAL

Fig. S1

**A**



**B**



# **Effects of triclocarban on the energetic content and gluconeogenic enzymes activity in the rat liver**

Vanesa de Oliveira Pateis<sup>1</sup>, Ana Paula Ames-Sibin<sup>1</sup>, Livia Bracht<sup>1</sup>, Adelar Bracht<sup>1</sup>, Jurandir F. Comar<sup>1\*</sup>

<sup>1</sup> Department of Biochemistry, State University of Maringa, PR, Brazil

Address for correspondence:

\*Jurandir Fernando Comar

Department of Biochemistry

University of Maringá

87020900 Maringá, Brazil

Email: [jfcomar@uem.br](mailto:jfcomar@uem.br)

Grant sponsor: Conselho Nacional de Desenvolvimento Científico e Tecnológico (CNPq); Grant number: 447876/2014-7

## ABSTRACT

Triclocarban (TCC) is a polychlorinated antimicrobial agent extensively used as antiseptic and preservative in personal care products, medical supplies and plastics. TCC orally administered triggers hepatotoxicity in mice and, *in vitro*, it negatively modify the respiration of isolated hepatic mitochondria. These actions impair gluconeogenesis and ammonia detoxification in the liver and they seem the consequence of a reduced energetic load of the organ. The latter was not yet determined in the liver. Therefore, this study investigated the actions of TCC on the hepatic content of ATP, ADP and AMP in perfused livers under gluconeogenic condition. The effects of TCC on activity of hepatic gluconeogenic key enzymes *in vitro* and the rate of TCC single-pass transformations in perfused livers were additionally determined. The livers of rats were perfused with Krebs-Henseleit bicarbonate buffer (pH 7.4) and TCC was infused at the concentrations range up to 75  $\mu$ M. The levels of TCC was measured in the inflowing and outflowing perfusion fluid and adenine mononucleotides in the freeze-clamped perfused livers by HPLC. TCC decreased the hepatic content of ATP by 38% and increased the content of AMP by 95%. The ADP content was not modified by TCC in the liver. TCC decreased the ratios of ATP/ADP and ATP/AMP by 42% and 70%, respectively. TCC did not modify the liver activity of G6Pase, FBPase-1 and PEPCK, however, the carboxylation of pyruvate was completely inhibited by the compound. The single-pass 25  $\mu$ M TCC through perfused livers shows that the compound is extensively retained and/or transformed in the organ (more than 90%) and this percentage is maintained or even increased when 75  $\mu$ M TCC is infused. The results show that TCC causes a great reduction of the energetic load of the liver, which can be due to the compound itself or its metabolites and should be the cause of the impaired hepatic gluconeogenesis.

**Keywords:** *triclocarban biotransformation, gluconeogenesis, pyruvate carboxylase, ATP content, liver perfusion, adenine nucleotides.*

## 4. INTRODUCTION

Triclocarban (TCC) is a polychlorinated aromatic compound extensively used as antimicrobial agent in various personal care products, including toothpaste, soaps, shampoo, antiperspirants [Iacopetta et al., 2021]. TCC is also used in medical settings and even in plastics, toys, clothing and food packaging materials [Iagopetta et al., 2021]. This biocide is absorbed into oral mucosa and skin and it is found in a number of human fluids, including urine, blood and seminal fluid [Halden et al., 2017; Buck Louis et al., 2018; Wei et al., 2017; Yin et al., 2016]. TCC has been associated with endocrine disruption and its uncontrolled use has been in addition related to bacterial resistance [Buck Louis et al., 2018; Halden et al., 2017; Kim & Rhee, 2016]. The adverse effects for human health led, in 2016, the US Food and Drug Administration (FDA) to prohibit all antibacterial soap products containing TCC [Food and Drug Administration, 2016]. However, TCC continues to be incorporated as preservative agent into a number of other personal care products in other countries and a large amount of the chemical is released into the environment causing bioaccumulation [Yun et al., 2020; Chen et al., 2019]. In spite of all evidences, many effects of TCC to humans remain controversial and require additional research.

The liver is involved in a number of physiological functions, including a pivotal role in body metabolic homeostasis [Sharabi et al., 2015]. The liver is also the most important organ for the biotransformation of drugs and it is exposed to xenobiotics during its metabolic functions [Gu & Manautou, 2012; Eler et al., 2013; Franco-Salla et al., 2019; Pateis et al., 2018]. In the liver, TCC is hydroxylated via phase I reactions by cytochrome P450 enzymes producing mainly 2'-OH-TCC, 6'-OH-TCC, 3',4'-dichloro-4-hydroxycarbanilide (DHC) and 3'-OH-TCC [Schebb et al., 2011; Zhang et al., 2020]. All these metabolites may undergo extensive phase II metabolism producing sulphates and glucuronides [Zhang et al., 2020]. The hydroxylated metabolites of TCC has been associated with hepatic cytotoxicity, mainly 6'-OH-TCC and 2'-OH-TCC, which present half-maximal effective concentration (EC<sub>50</sub>) values of 2.42 µM and 3.38 µM, respectively, in 48 h-treated hepatocytes [Zhang et al., 2020]. Therefore, TCC and its metabolites should certainly affect the energy-dependent metabolic fluxes in the organ. In fact, TCC has been reported to uncouple the

oxidative phosphorylation of rat liver isolated mitochondria and to trigger prooxidative damage in cultured hepatocytes [Xia et al., 2018; Zhang et al., 2020]. Metabolomics analysis also reveals that TCC orally administered to mice triggers hepatotoxicity and modifies the hepatic metabolism [Li et al., 2018].

We recently investigated the short-term actions of TCC in perfused rat livers and found that TCC produces significant effects on the hepatic energy metabolism at portal concentrations as low as 5  $\mu\text{M}$  [Pateis et al., 2022]. More precisely, TCC inhibited the liver gluconeogenesis and ammonia detoxification, which seem to be the consequence of an impaired mitochondrial metabolism. In fact, experimental approaches with isolated hepatic mitochondria have shown that in addition to an uncoupling action TCC inhibits the electron flow coupled to oxidative phosphorylation [Pateis et al., 2022]. Although TCC has reduced the efficiency of mitochondrial energy transduction, the real liver content of ATP in the presence of the drug has not been yet measured in the liver.

Evidences indicate that the actions on mitochondria are not the only ones responsible for the modifications caused by TCC on metabolic fluxes in perfused livers [Pateis et al., 2022]. This is because the liver gluconeogenesis from lactate and fructose were inhibited by TCC with  $\text{IC}_{50}$  values very similar (20  $\mu\text{M}$ ). However, gluconeogenesis from fructose should be inhibited in a lower extension than that from lactate if the reduced mitochondrial energetic support was the only cause. After all, fructose does not pass through the costly initial steps of gluconeogenesis within the mitochondria and, therefore, requires only one third of ATP than that from lactate [Simões et al., 2017]. An inhibition of gluconeogenic key enzymes, namely glucose-6-phosphatase and fructose-1,6-bisphosphatase, should not be excluded. Another possibility could be the hepatic metabolization of TCC, which could divert important amounts of reducing equivalents from gluconeogenesis to produce NADPH necessary for TCC hydroxylation. Oxidation of NADPH in consequence of biotransformation reactions affects biosynthetic pathways that depend on reducing power in the form of NADPH or NADH, such as gluconeogenesis [Scholz et al., 1973].

Considering all the above, the present study investigated (1) the actions of TCC on the levels of adenine mononucleotides (ATP, ADP and AMP) in perfused livers under gluconeogenic condition; (2) the effects of TCC on the activity of hepatic gluconeogenic key enzymes *in vitro*; and (3) the rate of TCC single-pass transformations in perfused livers.

## **5. MATERIALS AND METHODS**

### **5.1. Chemicals**

The rat liver perfusion apparatus was built in the workshops of the State University of Maringá (UEM), Brazil. Standard laboratory diet for rats was purchased from Nuvilab (Colombo, PR, Brazil). Triclocarban – TCC or 1-(4-chlorophenyl)-3-(3,4-dichlorophenyl)urea) – CAS number 101-20-2 and 99% purity, enzymes and coenzymes were purchased from Sigma Chemical Co (St. Louis, MO, USA). All other chemicals were of analytical grade.

### **5.2. Animals**

Male Wistar rats weighting 200-240 g (60 days old) were obtained from the Center of Animal Breeding of the State University of Maringá (UEM) and maintained under standard laboratory conditions at a temperature of  $24 \pm 2^{\circ}\text{C}$  under a regulated 12 hours light/dark cycle. The animals were housed in conventional steel cages (3 rats/cage) and fed ad libitum with a standard laboratory diet. After 3 days for acclimatization, animals were used for experiments. For preparing the liver for perfusion the rats were anesthetized by intraperitoneal injection of ketamine (90 mg/kg) and xylazine (9 mg/Kg). The procedures followed the guidelines of the Brazilian Council for the Control of Animal Experimentation (CONCEA) and were previously approved by the Ethics Committee for Animal Experimentation (CEUA) of the State University of Maringá (Protocol number CEUA 24391402018).

### **5.3. Liver perfusion and protocols**

Hemoglobin-free non-recirculating liver perfusion was performed as previously described [[Comar et al., 2003](#)]. Deeply anesthetized rats had the peritoneal cavity exposed and, after cannulation of the portal and cava veins, the liver was removed and positioned in a plexiglass chamber. The perfusion fluid was Krebs/Henseleit-bicarbonate buffer (pH 7.4) containing 25 mg% bovine serum albumin and saturated with a mixture of oxygen and carbon dioxide (95:5) by means of a membrane oxygenator with simultaneous temperature adjustment at  $37^{\circ}\text{C}$ . The flow was maintained constant by a peristaltic pump (Minipuls 3, Gilson, France). Oxygen consumption was

monitored by polarography.

Livers from fed rats were perfused with Krebs/Henseleit buffer to investigate the biotransformation of TCC. After stabilization of the oxygen consumption, TCC was infused at the concentrations of 25  $\mu\text{M}$  and 75  $\mu\text{M}$  during 20 minutes and by additional 10 minutes after ceasing the drug infusion. Samples of the outflowing perfusate were collected at five minutes intervals and analyzed by their contents of TCC.

For quantifying the hepatic content of adenine nucleotides the livers from 15 h fasted rats were perfused Krebs/Henseleit bicarbonate buffer under gluconeogenic conditions. After stabilization of the oxygen consumption, L-lactate (2 mM) was infused during 45 minutes perfusion time. TCC at the concentration of 75  $\mu\text{M}$  was introduced from 25 minutes perfusion time. At 45 min perfusion time, the livers were immediately clamped in liquid nitrogen for adenine nucleotides assessment.

#### **5.4. Hepatic content of adenine mononucleotides**

The hepatic content of the adenine mononucleotides was measured after freeze-clamping the perfused livers with liquid nitrogen. ATP, ADP and AMP were extracted from the freeze tissue with 0.6 M perchloric acid and their contents determined by high-performance liquid chromatography (HPLC) analysis [Wendt et al., 2019]. The HPLC system (Shimadzu, Japan) consisted of a system controller (SCL-10AVP), two pumps (model LC10ADVP), a column oven (model CTO-10AVP) and an UV-Vis detector (model SPD-10AV). A reversed-phase C18 CLC-ODS column (5  $\mu\text{m}$ , 250 $\times$ 4.6 mm i.d.; Shimadzu) protected with a CLC-ODS precolumn (5  $\mu\text{m}$ , 4 $\times$ 3 mm i.d.; Phenomenex), was used with a gradient from reversed-phase 0.044  $\text{M}\cdot\text{L}^{-1}$  phosphate buffer solution (PBS; pH 6.0) to 0.044  $\text{M}\cdot\text{L}^{-1}$  PBS plus methanol (1:1; pH 7.0). In percent methanol, the gradient was the following: at 0 min, 0%; at 2.5 min, 0.5%; at 5 min, 3%; at 7 min, 5%; at 8 min, 12%; at 10 min, 15%; at 12 min, 20%; at 20 min, 30%. The temperature was kept at 35  $^{\circ}\text{C}$ , and the injection volume was 20  $\mu\text{L}$  with a flow rate of 0.8 mL/min. Monitoring was performed spectrophotometrically at 254 nm. Identification of the peaks of ATP, ADP and AMP was carried out by a comparison of their retention times with those obtained by injecting standards under the same conditions. The concentrations of the compounds were

calculated by means of the regression parameters obtained from the calibration curves constructed with standard solutions. Linear relationships were obtained between the concentrations and the areas under the elution curves.

### **5.5. Hepatic TCC transformation**

The transformation of TCC was evaluated in perfused livers of fed rats as previously described [[Pereira-Maróstica et al., 2022](#)]. The content of TCC in the inflowing and outflowing perfusion fluid were measured by high-performance liquid chromatography (HPLC). The HPLC system was that used for adenine mononucleotide quantification. A reversed-phase C18 CLC-ODS column (5 µm, 250 × 4.6 mm i.d.; Shimadzu) protected with a CLC-ODS precolumn (5 µm, 4 × 3 mm i.d.; Phenomenex), was used with a mobile isocratic reversed-phase composed of methanol-acetonitrile-phosphate buffer (15:15:75, v/v; pH 6.3). The injected sample volume was 20 µL and the flow remained constant at 1.0 mL/min. Monitoring was performed with an ultraviolet detector set at 270 nm. The peaks were identified through the retention times collected by the injection of the TCC standard at the same conditions, being 8-9 minutes. The concentrations of the compounds were calculated by means of the regression parameters obtained from the calibration curves constructed with standard solutions. Linear relationships were obtained between the concentrations and the areas under the elution curves.

### **5.6. Mitochondria and microsomes isolation**

Mitochondria were isolated by differential centrifugation as previously described [[Biazon et al., 2016](#)]. Briefly, anesthetized rats had the peritoneal cavity exposed, the liver removed and placed in ice-cold buffer containing 200 mM mannitol, 75 mM sucrose, 0.2 mM ethylene glycol tetraacetic acid (EGTA), 2 mM tris(hydroxymethyl)amino-methane (Tris-HCl), pH 7.4 and 50 mg% bovine serum albumin. The organ was minced, washed and homogenized in the same medium with a Van Potter-Elvehjem homogenizer. The homogenate was then centrifuged sequentially at 600 g (10 min) and 7000 g (10 min). The pellet with the intact mitochondria was washed twice and resuspended with the buffer without EDTA. The protein content in the mitochondrial fraction was measured using the Folin phenol reagent. Hepatic mitochondria and microsomes were

isolated by differential centrifugation [Vilela et al., 2014; Biazon et al., 2016].

Hepatic microsomes were isolated by differential centrifugation as previously described [Vilela et al., 2014]. Briefly, anesthetized rats had the peritoneal cavity exposed, the liver removed and placed in a isolation medium containing 150 mM KCl, 0.1 mM phenylmethanesulfonyl-fluoride (PMSF) and 10 mM Tris-HCl (pH 7.4). The liver was then minced, washed and homogenized in the same medium with a Van Potter-Elvehjem homogenizer. The homogenate was centrifuged at 2550g for 10 min and the supernatant again centrifuged in two steps of 7100g and 12400g for 10 minutes. Finally, the supernatant of the last centrifugation was centrifuged at 105,000g for 1 hour. The pellet containing the microsomal fraction was suspended in cold isolation medium at a final protein concentration of 20 mg/mL. The remaining supernatant was separated as soluble cytosolic fraction of the liver.

### **5.7. Hepatic gluconeogenic enzymes assays**

The activity of glucose 6-phosphatase (G6Pase) was measured in isolated microsomes by the spectrophotometric quantification of the released phosphate from glucose 6-phosphate [Vilela et al., 2014]. Briefly, the incubation medium (1.1 mL) contained 100 mM KCl, 5 mM MgCl<sub>2</sub>, 20 mM Tris-HCl (pH 7.2), 15 mM glucose 6-phosphate and 0.1–0.2 mg microsomal protein. TCC was added to this medium at various concentrations in the range up to 200 μM. After 20 min incubation at 37 °C, the reaction was stopped by the addition of one volume of 5% trichloroacetic acid (TCA) and phosphate release was measured. Rates were expressed as μmol/(min x mg protein).

The activity of hepatic fructose 1,6-bisphosphatase (FBPase-1) was determined using the supernatant from the centrifugation at 105,000g that was obtained during the isolation procedure of the microsomal fraction. The FBPase-1 activity was measured by the quantification of released phosphate from fructose-1,6-bisphosphate [Lima et al., 2006]. The reaction mixture contained supernatant at approximately 1 mg protein/mL, 100 mM tris-HCl (pH 8), 12 mM MgCl<sub>2</sub>, 1 mM D-fructose 1 and 5 mM cysteine. After 20 min incubation at 37 °C, the reaction was interrupted by the addition of one volume of 5% TCA and phosphate release was measured by spectrophotometry.

The activity of hepatic phosphoenolpyruvate carboxykinase (PEPCK) were

determined using the supernatant from the centrifugation at 105,000g that was obtained during the isolation procedure of the microsomal fraction. The PEPCK activity was estimated by coupling the malate dehydrogenase to the PEPCK reaction [Petersen et al., 2001]. The assay medium contained 50 mM HEPES buffer (pH 7.0), 100  $\mu$ M MnCl<sub>2</sub>, 5 mM MgCl<sub>2</sub>, 20 mM KHCO<sub>3</sub>, 2 mM reduced glutathione, 0.2 mM NADH, 2 mM phosphoenolpyruvate, 100  $\mu$ M GDP and 8.7 units/ml L-malate dehydrogenase. TCC was added to this medium at various concentrations in the range up to 200  $\mu$ M. The oxidation of NADH by oxaloacetate formed in the PEPCK reaction was assayed spectrophotometrically at 340 nm and the activity was expressed as  $\mu$ mol/(min x mg protein).

The effect of TCC on the pyruvate carboxylase activity was indirectly assayed by measuring the incorporation of <sup>14</sup>C from [<sup>14</sup>C]NaHCO<sub>3</sub> into components of the tricarboxylic acid cycle by freshly isolated intact mitochondria [Lima et al., 2006]. The incubation medium contained 5 mM pyruvate, 12.5 mM MgCl<sub>2</sub>, 2.5 mM potassium phosphate, 120 mM KCl, 10 mM HEPES (pH 7.5), and 3 mg protein/mL of freshly isolated intact mitochondria. TCC was added to this medium at various concentrations in the range up to 200  $\mu$ M. The reaction was initiated by introducing 12 mM [<sup>14</sup>C]NaHCO<sub>3</sub> (0.25  $\mu$ Ci). After 10 min of incubation at 37 °C under constant agitation, the reaction was arrested by the addition of a 0.5 volumes of 2 M perchloric acid. After expulsion of the remaining [<sup>14</sup>C]NaHCO<sub>3</sub> (5 min), aliquots were taken for counting the acid stable incorporated radioactivity by liquid scintillation spectrometry (TriCarb 2810 TR counter, Perkin Elmer). The results were expressed as nmol/(min x mg protein). The following scintillation solution was used: toluene/ethanol (2:1) containing 5 g/L 2,5-diphenyloxazole and 0.15 g/L 2,2-p-phenylenebis(5-phenyloxazole).

## 5.8. Statistical analysis

The parameters presented in graphs and tables are means  $\pm$  standard errors of the means. Statistical analysis and area under the curve calculation were done by means of the GraphPad Prism Software (version 8.0). The statistical significance of the data was analyzed by means of ANOVA TWO-WAY and the Newman-Keuls post-hoc test was applied with the 5% level of significance (p<0.05). For comparison of two values the student t test was applied with the 5% level (p<0.05).

## 6. RESULTS AND DISCUSSION

### 6.1. Hepatic content of adenine mononucleotides

The real hepatic energetic load was accessed measuring directly the contents of adenine mononucleotides, namely ATP, ADP and AMP, in perfused livers under gluconeogenic conditions in the absence and presence of TCC. L-lactate was used as gluconeogenic precursor and TCC was infused at the concentration of 75  $\mu\text{M}$ . The latter completely inhibits gluconeogenesis in perfused rat liver [Pateis et al., 2022]. Fig 1 shows the hepatic contents of ATP, ADP and AMP (Panel A) and the ratios of ATP/ADP and ATP/AMP (Panel B). TCC decreased the hepatic content of ATP by 38% and increased the content of AMP by 95%. The ADP content was not modified by TCC in the liver. TCC decreased the ratios of ATP/ADP and ATP/AMP by 42% and 70%, respectively. The reduced energetic apport in the liver must be certainly the consequence of an impaired mitochondrial oxidative phosphorylation caused by TCC, which has been reported to act as an uncoupler agent and as an inhibitor of the coupled electron flow at the mitochondrial level [Pateis et al., 2022]. The results also corroborate reports in which TCC perturbs the ATP metabolism in cultured hepatocytes and also uncouples the oxidative phosphorylation of rat liver isolated mitochondria [Xia et al., 2018; Zhang et al., 2020]. In addition, the lower ATP content is probably the main reason by which TCC inhibits the costly gluconeogenesis and ammonia detoxification in perfused rat livers [Pateis et al., 2022].

### 6.2. Gluconeogenic key enzymes activity

Considering that TCC inhibited in perfused livers equally gluconeogenesis from lactate and fructose, which require different energetic apport, an additional inhibition of gluconeogenic enzymes should not be excluded. For this reason, *in vitro* assays were carried out to evaluate the effect of TCC on activity of the key gluconeogenic enzymes G6Pase, FBPase-1, PEPCK and pyruvate carboxylation. The results are shown in Fig. 2. As noted, TCC at all concentrations tested did not modified the liver activity of G6Pase, FBPase-1 and PEPCK, except by a slightly stimulation in the G6Pase activity at the concentration of 20  $\mu\text{M}$  (Fig. 2A, B and C). On the other hand, the carboxylation of pyruvate was completely inhibited by TCC at the concentrations of 50, 100 and 200  $\mu\text{M}$  (Fig. 2D). The

pyruvate carboxylase catalyzes the carboxylation of pyruvate into the mitochondria in a process that requires substantial energy input in a form of ATP. In the present study the activity of this enzyme was determined indirectly by the carboxylation of pyruvate in intact phosphorylating mitochondria. In this assay the organelle must respire and produce the ATP used to carboxylate the pyruvate. Thus, an inhibition of pyruvate carboxylation can be attributed not only by a direct enzyme inhibition, but also by factors that affect the reaction, as for example, the pyruvate transport into mitochondria or an impairment of mitochondrial ATP synthesis. The latter, however, should be the main reason because the liver ATP content was considerably decreased and mitochondrial oxidative phosphorylation is impaired by TCC. On the other hand, it is not possible to conclude that TCC does not have modified the activity of other enzymes in the perfused livers. This is especially true if one considers that these enzymes are also under allosteric control. The latter phenomenon possibly played a significant role in the overall effects of TCC, as suggested by the modifications induced by the compound, for example, in the allosterically important ADP/ATP and AMP/ATP ratios.

### **6.3. Single-pass TCC transformation**

Many effects of TCC on liver metabolism showed a complex pattern, more specifically it inhibited the costly gluconeogenesis and stimulated the oxygen consumption in perfused livers, while it simultaneously uncoupled oxidative phosphorylation and inhibited the state III respiration of isolated mitochondria [Pateis et al., 2022]. These opposite effects could be the result of the transformations of TCC in the liver and, consequently, the effect of different compounds in the organ. Evaluation of the single-pass transformation of TCC is important because it allows to infer about the concentration gradient and transformations of the compound along the sinusoids, which in turn is likely to affect its activity in the liver as a whole. For this purpose, TCC was infused during 20 min in perfused livers at the concentrations of 25 and 75  $\mu\text{M}$ , which strongly inhibits the glucose production from various substrates and, in addition, exhibits the previously mentioned behavior of stimulus of oxygen consumption in perfused livers and inhibition of oxygen consumption in isolated mitochondria [Pateis et al., 2022]. Liver of fed rats were used because glycogenolysis should

provide glucose for glucuronidation reactions. The latter should accelerate the TCC transformations in the liver because glucuronidation is an important step of this drug metabolism [Schebb et al., 2011; Zhang et al., 2020]. Samples of the inflowing and outflowing perfusion fluid were analyzed for their content of TCC by HPLC. Fig. 3A illustrates a typical chromatogram of the inflowing perfusate with TCC at the concentration of 25  $\mu\text{M}$  ( $74.30 \text{ ng}\cdot\text{min}^{-1}\cdot\text{g}^{-1}$ ), monitored at 270 nm, which shows a single significant peak appearing at 9.2 min and that is attributable to TCC. Prolongation of the separation time of 12 min shown in Fig. 3A for more 40 min did not reveal any further component absorbing at 270 nm. When the outflowing perfusate was analyzed, the profile changed enormously and that peak at 9.2 min was very strongly reduced (Panels B and C in Fig. 3). The degree of this reduction can be noticed by comparing the scale of Panel A with the scales in Panels B, C and D, which were expanded by a factor of 10, approximately. Actually, the concentration of TCC in the outflowing perfusate reached 2.09  $\mu\text{M}$  ( $6.21 \text{ ng}\cdot\text{min}^{-1}\cdot\text{g}^{-1}$ ) after 1 min infusion and increased to 9.10  $\mu\text{M}$  ( $27.03 \text{ ng}\cdot\text{min}^{-1}\cdot\text{g}^{-1}$ ) after 20 min infusion. Even 10 min after ceasing the TCC infusion its concentration in the outflowing perfusate reaches 3.24  $\mu\text{M}$  ( $9.62 \text{ ng}\cdot\text{min}^{-1}\cdot\text{g}^{-1}$ ) (Panels D in Fig. 3).

Fig. 4 shows the time courses of TCC output in perfused liver caused by the infusion of the compound at the concentration of 25  $\mu\text{M}$  (Panel A) and 75  $\mu\text{M}$  (Panel B). Fig. 4 also illustrate the experimental protocol. TCC was infused during 20 min and by additional 10 minutes after ceasing the drug infusion. Samples of the outflowing perfusate were collected at five minutes intervals and analyzed by their contents of TCC. Fig. 4 illustrates only the perfusion time from that moment in which TCC is introduced in the liver. Upon 25  $\mu\text{M}$  TCC infusion, the levels of the compound progressively increased in the outflowing perfusate until 15 minutes perfusion time, when achieved a steady-state (Fig. 4A). When its introduction was interrupted, the hepatic output of TCC rapidly decreased, but not completely, at least until 10 min after. Upon 75  $\mu\text{M}$  TCC infusion, the levels of the compound immediately increased in the outflowing perfusate at values that were maintained until 20 min perfusion time, when its introduction was interrupted (Fig. 4B). After this period, the hepatic output of TCC decreases, but at a lower rate when compared with 25  $\mu\text{M}$  TCC.

The rates of TCC releases in Fig 4A and B (0-30 min) can be best appreciated by evaluating the area under the curve (AUC), which corresponds

to the total amounts released during this period. [Table 1](#) shows the total amounts of TCC introduced during 20 min and the total amount released during 30 min, both expressed as  $\mu\text{mol/g}$  liver. [Table 1](#) also shows the total amount of TCC that was did not appear in the outflowing perfusate until 30 min perfusion time. The latter was calculated by the subtraction of TCC in the outflowing perfusate (AUC: 0-30 minutes) from the total amount introduced during 20 min and it is sum of TCC that was transformed and that retained in the organ. It is possible to extracted two important information from [Table 1](#): TCC is extensively retained or transformed in the liver (more than 90% of the infused TCC) and this percentage is maintained or even increased when TCC is infused at the higher concentration (75  $\mu\text{M}$ ).

It is very difficult to distinguish between the amount of TCC that was retained and that transformed in the liver, however, both phenomena should be associated with the negative effects of the compound. If TCC is mainly retained in the liver, its parenchymal concentration is greatly increased and this bioaccumulation in the organ could be responsible by the negative effects. On the other hand, if TCC is mainly transformed in the liver, its metabolites, particularly 6'-OH-TCC and 2'-OH-TCC, are also associated with high toxicity against hepatocytes [[Zhang et al., 2020](#)] and should certainly affect the energy-dependent metabolic fluxes in the organ. In this regard, even if TCC is poorly transformed in the liver, the half-maximal effective concentration ( $\text{EC}_{50}$ ) values of the two main metabolites is relatively low: 2.42  $\mu\text{M}$  and 3.38  $\mu\text{M}$ , respectively, for 6'-OH-TCC and 2'-OH-TCC [[Schebb et al., 2011](#); [Zhang et al., 2020](#)]. On the other hand, the effects on isolated mitochondria previously reported [[Pateis et al., 2022](#); [Xia et al., 2018](#)] is probably caused by TCC itself. This because TCC transformations occur mainly at the microsomal levels, which is not present in the incubation system, at least in significative amounts [[Iacopetta et al., 2021](#)]. Herein, the single-pass TCC transformation in perfused livers provides only preliminary results and to understand if the compound is mainly transformed or retained in the organ still requires additional approaches. However, the results show that TCC itself or in association with its metabolites cause a great reduction of the ATP content in the rat liver, particularly under gluconeogenic conditions, and this effect should be the cause of the impaired hepatic gluconeogenesis.

## **CONCLUSION**

The infusion of TCC in perfused rat livers greatly decreases the content of ATP, increases the content of AMP and decreases the ratios ATP/ADP and ATP/AMP. The impairment of mitochondrial oxidative phosphorylation should be the cause of these effects. In addition, TCC completely inhibits the carboxylation of pyruvate in the coupled phosphorylating mitochondria and the ATP deficiency should be the reason. The single-pass TCC through perfused liver shows that substantial amount of TCC is transformed and/or retained in the organ and the phenomenon could be associated with the negative effects of TCC in the liver. These evidences should give more support for regulatory health agencies to prohibit personal care products containing TCC or at least to consider a more deeply evaluation of acute toxicity of the drug.

## **Acknowledgements**

Authors wish to thank the financial support of the Coordenação de Aperfeiçoamento de Pessoal de Nível Superior (CAPES) and of the Conselho Nacional de Desenvolvimento Científico e Tecnológico (CNPq).

## **Competing interests**

The authors declare that no competing interest exists and that all approved the final manuscript.

## REFERENCES

- Biazon ACB, Wendt MNM, Moreira JR, Ghizoni CVC, Soares AA, Silveira SS, Sá-Nakanishi AB, Amado CAB, Peralta RM, Bracht A, Comar JF. The in vitro antioxidant capacities of hydroalcoholic extracts from roots and leaves of *Smallanthus sonchifolius* (Yacon) do not correlate with their in vivo antioxidant action in diabetic rats. *J. Biosci Med* 4:15-27. [Doi: 10.4236/jbm.2016.42003](https://doi.org/10.4236/jbm.2016.42003)
- Buck Louis GM, Smarr MM, Sun L, Chen Z, Honda M, Wang W, Karthikraj R, Weck J, Kannan K. Endocrine disrupting chemicals in seminal plasma and couple fecundity. *Environ Res* 2018; 163:64-70. [Doi: 10.1016/j.envres.2018.01.028](https://doi.org/10.1016/j.envres.2018.01.028)
- Chen J, Meng XZ, Bergman A, Halden RU. Nationwide reconnaissance of five parabens, triclosan, triclocarban and its transformation products in sewage sludge from China. *J Hazard Mater* 2019; 365:502-510. [Doi: 10.1016/j.jhazmat.2018.11.021](https://doi.org/10.1016/j.jhazmat.2018.11.021)
- Comar JF, Suzuki-Kemmelmeier F, Bracht A. The action of oxybutinin on haemodynamics and metabolism in the perfused rat liver. *Basic Clin Pharmacol Toxicol* 2003; 93:147-152. [Doi:10.1034/j.1600-0773.2003.930307.x](https://doi.org/10.1034/j.1600-0773.2003.930307.x)
- Eler GJ, Santos IS, de Moraes AG, Mito MS, Comar JF, Peralta RM, Bracht A. Kinetics of the transformation of n-propyl gallate and structural analogs in the perfused rat liver. *Toxicol Appl Pharmacol* 2013; 273:35-46. [Doi: 10.1016/j.taap.2013.08.026](https://doi.org/10.1016/j.taap.2013.08.026)
- Food and Drug Administration, HHS. Safety and Effectiveness of Consumer Antiseptics; Topical Antimicrobial Drug Products for Over-the-Counter Human Use. Final rule. *Fed Regist.* 2016; 81(172):61106-61130. [PMID: 27632802](https://pubmed.ncbi.nlm.nih.gov/27632802/)
- Franco-Salla GB, Bracht L, Parizotto AV, Comar JF, Peralta RM, Bracht F, Bracht A. Kinetics of the metabolic effects, distribution spaces and lipid-bilayer affinities of the organo-chlorinated herbicides 2,4-D and picloram in the liver. *Toxicol Lett* 2019; 313:137-149. [Doi: 10.1016/j.toxlet.2019.06.008](https://doi.org/10.1016/j.toxlet.2019.06.008)
- Gu X, Manautou JE. Molecular mechanisms underlying chemical liver injury. *Expert Rev Mol Med.* 2012 14:e4. [Doi: 10.1017/S1462399411002110](https://doi.org/10.1017/S1462399411002110)
- Halden RU, Lindeman AE, Aiello AE, Andrews D, Arnold WA, Fair P, Fuoco RE, Geer LA, Johnson PI, Lohmann R, McNeill K, Sacks VP, Schettler T, Weber R, Zoeller RT, Blum A. The florence statement on triclosan and triclocarban. *Environ Health Perspect* 2017; 125:064501. [Doi: 10.1289/EHP1788](https://doi.org/10.1289/EHP1788)
- Iacopetta D, Catalano A, Ceramella J, Saturnino C, Salvagno L, Ielo I, Drommi D, Scali E, Plutino MR, Rosace G, Sinicropi MS. The different facets of triclocarban: a review. *Molecules* 2021; 26:2811. [Doi: 10.3390/molecules26092811](https://doi.org/10.3390/molecules26092811)
- Kim SA, Rhee MS. Microbicidal effects of plain soap vs triclocarban-based antibacterial soap. *J Hosp Infect* 2016; 94:276-280. [Doi: 10.1016/j.jhin.2016.07.010](https://doi.org/10.1016/j.jhin.2016.07.010)
- Li W, Zhang W, Chang M, Ren J, Xie W, Chen H, Zhang Z, Zhuang X, Shen G, Li H. Metabonomics reveals that triclocarban affects liver metabolism by affecting glucose metabolism,  $\beta$ -oxidation of fatty acids, and the TCA cycle in male mice. *Toxicol Lett* 2018; 299:76-85. [Doi: 10.1016/j.toxlet.2018.09.011](https://doi.org/10.1016/j.toxlet.2018.09.011)

Lima LC, GD Buss, EL Ishii-Iwamoto, CL Salgueiro-Pagadigorria, JF Comar, A Bracht, J Constantin, Metabolic effects of p-coumaric acid in the perfused rat liver. *J Biochem Mol Toxicol* 2006; 20:18-26. [Doi: 10.1002/jbt.20114](https://doi.org/10.1002/jbt.20114)

Pateis VO, Bracht L, Castro LS, Franco-Salla GB, Comar JF, Parizotto AV, Peralta RM, Bracht A. The food additive BHA modifies energy metabolism in the perfused rat liver. *Toxicol Lett* 2018; 299:191-200. [Doi: 10.1016/j.toxlet.2018.10.005](https://doi.org/10.1016/j.toxlet.2018.10.005)

Pateis VO, Ames-Sibin AP, Sá-Nakanishi AB, Bracht L, Bracht A, Comar JF. Short-term effects of the antimicrobial agent triclocarban on the energetic metabolism of rat liver. *Toxicol Appl Pharmacol* (2022), submitted.

Pereira-Maróstica HV, Bracht L, Comar JF, Peralta RM, Bracht A, Sá-Nakanishi AB. The rapid transformation of triclosan in the liver reduces its effectiveness as inhibitor of hepatic energy metabolism. *Toxicol Appl Pharmacol* 2022; 442:115987. [Doi: 10.1016/j.taap.2022.115987](https://doi.org/10.1016/j.taap.2022.115987)

Petersen S, Mack C, de Graaf AA, Ridel C, Eikmanns BJ, Sahm H. Metabolic consequences of altered phosphoenolpyruvate carboxikinase activity in *Corynebacterium glutamicum* reveal anaplerotic regulation mechanism in vivo. *Metab Eng* 2001; 3:344-361. [DOI: 10.1006/mben.2001.0198](https://doi.org/10.1006/mben.2001.0198)

Sharabi K, Tavares CDJ, Rines AK, Puigserver P. Molecular pathophysiology of hepatic glucose production. *Mol Aspects Med* 2015; 46:21-33. [Doi: 10.1016/j.mam.2015.09.003](https://doi.org/10.1016/j.mam.2015.09.003)

Schebb NH, Inceoglu B, Ahn KC, Morisseau C, Gee SJ, Hammock BD. Investigation of human exposure to triclocarban after showering and preliminary evaluation of its biological effects. *Environ Sci Technol* 2011; 45:3109-3115. [Doi: 10.1021/es103650m](https://doi.org/10.1021/es103650m)

Scholz R, Hansen W, Thurman RG. Interaction of mixed-function oxidation with biosynthetic processes. 1. Inhibition of gluconeogenesis by aminopyrine in perfused rat liver. *Eur J Biochem* 1973; 38:64-72. [Doi: 10.1111/j.1432-1033.1973.tb03034.x](https://doi.org/10.1111/j.1432-1033.1973.tb03034.x)

Simões MS, Bracht L, Parizotto AV, Comar JF, Peralta RM, Bracht A. The metabolic effects of diuron in the rat liver. *Environ Toxicol Pharmacol* 2017; 54:53-61. [Doi: 10.1016/j.etap.2017.06.024](https://doi.org/10.1016/j.etap.2017.06.024)

Vilela VR, Oliveira AL, Comar JF, Peralta RM, Bracht A. Effects of tadalafil on the cAMP stimulated glucose output in the rat liver. *Chem Biol Interact* 2014; 220: 1-11. [Doi: 10.1016/j.cbi.2014.05.020](https://doi.org/10.1016/j.cbi.2014.05.020)

Wei L, Qiao P, Shi Y, Ruan Y, Yin J, Wu Q, Shao B. Triclosan/triclocarban levels in maternal and umbilical blood samples and their association with fetal malformation. *Clin Chim Acta* 2017; 466:133-137. [Doi: 10.1016/j.cca.2016.12.024](https://doi.org/10.1016/j.cca.2016.12.024)

Wendt MNM, de Oliveira MC, Castro LS, Franco-Salla GB, Parizotto AV, Silva FMS, Natali MRM, Bersani-Amado CA, Bracht A, Comar JF. Fatty acids uptake and oxidation are increased in the liver of rats with adjuvant-induced arthritis.

Biochim Biophys Acta (BBA) Mol Basis Dis 2019; 1865:696-707. Doi: [10.1016/j.bbadis.2018.12.019](https://doi.org/10.1016/j.bbadis.2018.12.019)

Xia M, Huang R, Shi Q, Boyd WA, Zhao J, Sun N, Rice JR, Dunlap PE, Hackstadt AJ, Bridge MF, Smith MV, Dai S, Zheng W, Chu PH, Gerhold D, Witt KL, DeVito M, Freedman JH, Austin CP, Houck KA, Thomas RS, Paules RS, Tice RR, Simeonov A. Comprehensive analyses and prioritization of Tox21 10K chemicals affecting mitochondrial function by in-depth mechanistic studies. Environ Health Perspect 2018; 126:077010. Doi: [10.1289/EHP2589](https://doi.org/10.1289/EHP2589)

Yin J, Wei L, Shi Y, Zhang J, Wu Q, Shao B. Chinese population exposure to triclosan and triclocarban as measured via human urine and nails. Environ Geochem Health 2016; 38:1125-1135. Doi: [10.1007/s10653-015-9777-x](https://doi.org/10.1007/s10653-015-9777-x)

Yun H, Liang B, Kong D, Li X, Wang A. Fate, risk and removal of triclocarban: A critical review. J Hazard Mater 2020; 387:121944. Doi: [10.1016/j.jhazmat.2019.121944](https://doi.org/10.1016/j.jhazmat.2019.121944)

Zhang H, Lu Y, Liang Y, Jiang L, Cai Z. Triclocarban-induced responses of endogenous and xenobiotic metabolism in human hepatic cells: Toxicity assessment based on nontargeted metabolomics approach. J Hazard Mater 2020; 392:122475. Doi: [10.1016/j.jhazmat.2020.122475](https://doi.org/10.1016/j.jhazmat.2020.122475)

**TABLE 1.** *Single-pass transformation of TCC in perfused livers of rats.* Livers from fed rats were perfused with TCC as illustrated in Fig 4. TCC was quantified in the inflowing and outflowing perfusion fluid by HPLC. TCC inflow is expressed as AUC (0-20 minutes;  $\mu\text{mol}\cdot\text{g}^{-1}$ ) and corresponded to the average of total amount introduced in the liver. TCC output is expressed as AUC (0-30 minutes) and corresponded to the average mean of the total amount of TCC released in the outflowing perfusion fluid. The retained plus transformed TCC is the average mean and percentage obtained by subtracting TCC output (AUC: 0-30 minutes) from the TCC introduced in the liver. Data are the mean  $\pm$  SEM obtained from 5 animals for each condition.

Parameter	TCC inflow (AUC: 0→20 min)	TCC output (AUC: 0→30 min)	TCC retained + transformed (AUC: 0→30 min)	TCC retained + transformed
TCC	$\mu\text{mol}\cdot\text{g}^{-1}$	$\mu\text{mol}\cdot\text{g}^{-1}$	$\mu\text{mol}\cdot\text{g}^{-1}$	% of TCC inflowed
25 $\mu\text{M}$ TCC	1.50 $\pm$ 0.02	0.136 $\pm$ 0.006	1.368 $\pm$ 0.070	91.2
75 $\mu\text{M}$ TCC	4.50 $\pm$ 0.06	0.092 $\pm$ 0.005	4.408 $\pm$ 0.028	98.0

## FIGURE CAPTIONS

**Fig. 1.** *The effects of TCC on the contents of adenine mononucleotides in the perfused liver (A) and the ratios of ATP/ADP and ATP/AMP (B).* Livers from fasted rats were perfused with Krebs/Henseleit buffer as described in the section 2.3. After stabilization of the oxygen consumption, Lactate (2 mM) was infused during 45 minutes. For TCC group, this compound at the concentration of 75  $\mu\text{M}$  was introduced from 25 minutes perfusion time. At 45 min perfusion time, the livers were immediately clamped in liquid nitrogen and adenine nucleotides were extracted with cold perchloric acid. ATP, ADP and AMP were quantified by HPLC. Values are means  $\pm$  SEM. \* $p < 0.05$ : different from 0.0  $\mu\text{M}$  TCC (unpaired t test).

**Fig. 2.** *The effects of TCC on the activity of gluconeogenic key enzymes in the livers.* TCC was added to the incubation medium at the final concentrations of 10, 20, 50, 100 and 200  $\mu\text{M}$ . The enzymes activities are expressed per mg protein. PEPCCK: phosphoenol-pyruvate carboxykinase; FBPase-1: fructose 1,6-biphosphatase 1; G6Pase: glucose 6-phosphatase. Data are the mean  $\pm$  SEM of 4 animals. \* $p < 0.05$ : different from 0.0  $\mu\text{M}$  TCC.

**Fig. 3.** *Typical chromatograms of the perfusion fluid during TCC infusion.* Livers from fed rats were perfused with TCC (25 and 75  $\mu\text{M}$ ) during 20 min and samples of the outflowing perfusate were collected at 5 min intervals for HPLC analyses. The chromatogram shown in panel A corresponds to the inflowing perfusate and those shown in panels B and C refer to the outflowing perfusate at 1 and 20 min after starting infusion. The chromatogram shown in panel D corresponds to the outflowing perfusate at 10 min after ceasing TCC infusion.

**Fig. 4.** *Time courses of TCC release in the outflowing perfusate from livers perfused with the compound at the concentration of 25  $\mu\text{M}$  (Panel A) and 75  $\mu\text{M}$  (Panel B).* Livers from fed rats were perfused with Krebs/Henseleit buffer as described in the Section 2.3. TCC was infused during 20 min and the liver was perfused by additional 10 min after ceasing TCC infusion. Samples of the outflowing perfusate were collected at five min intervals and analyzed for their content of TCC by HPCL. The results are expressed as  $\eta\text{mol}\cdot\text{min}^{-1}\cdot\text{g}^{-1}$  and are the mean  $\pm$  SEM obtained from 5 animals.

Fig. 1

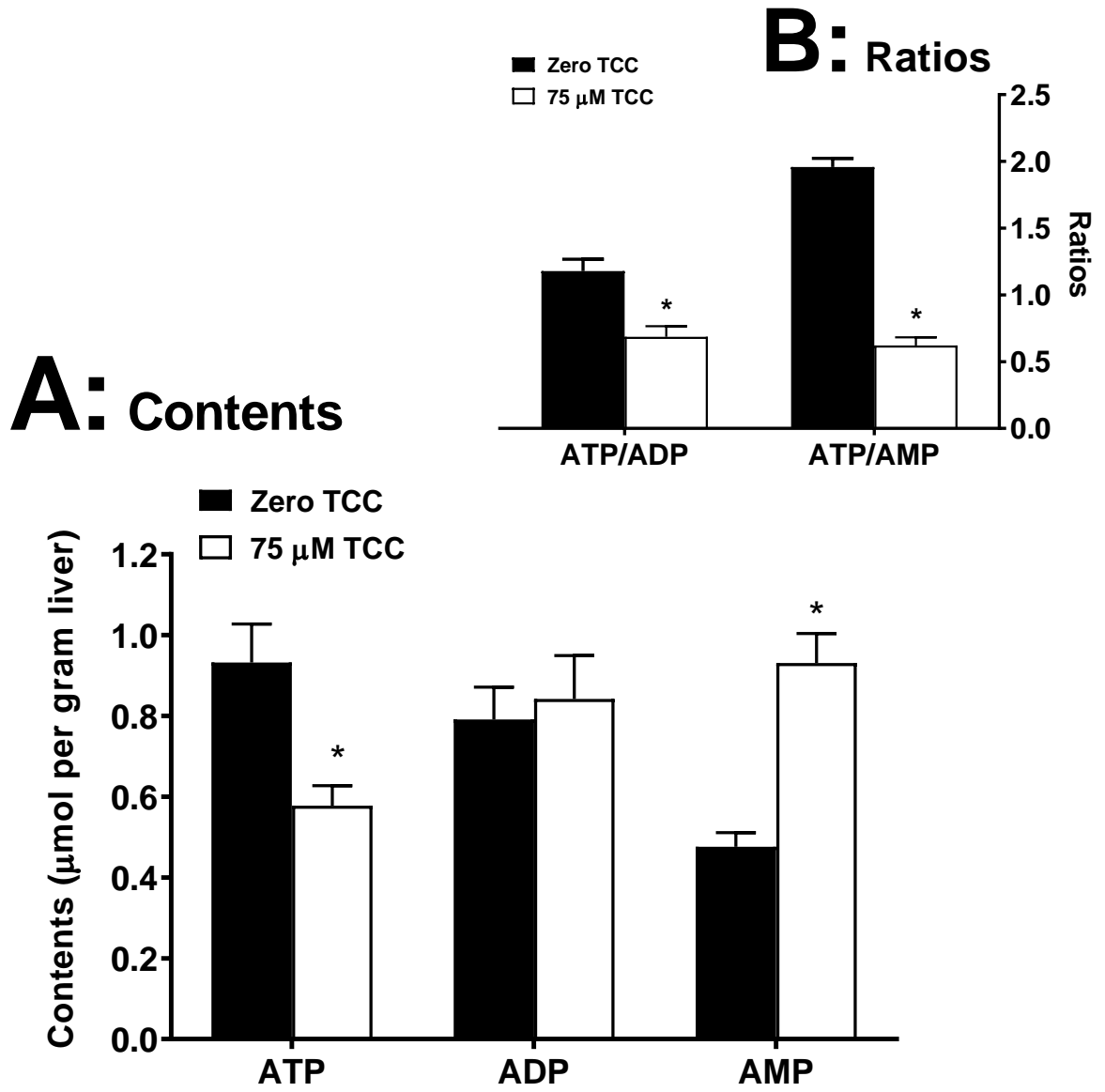


**Fig. 2**

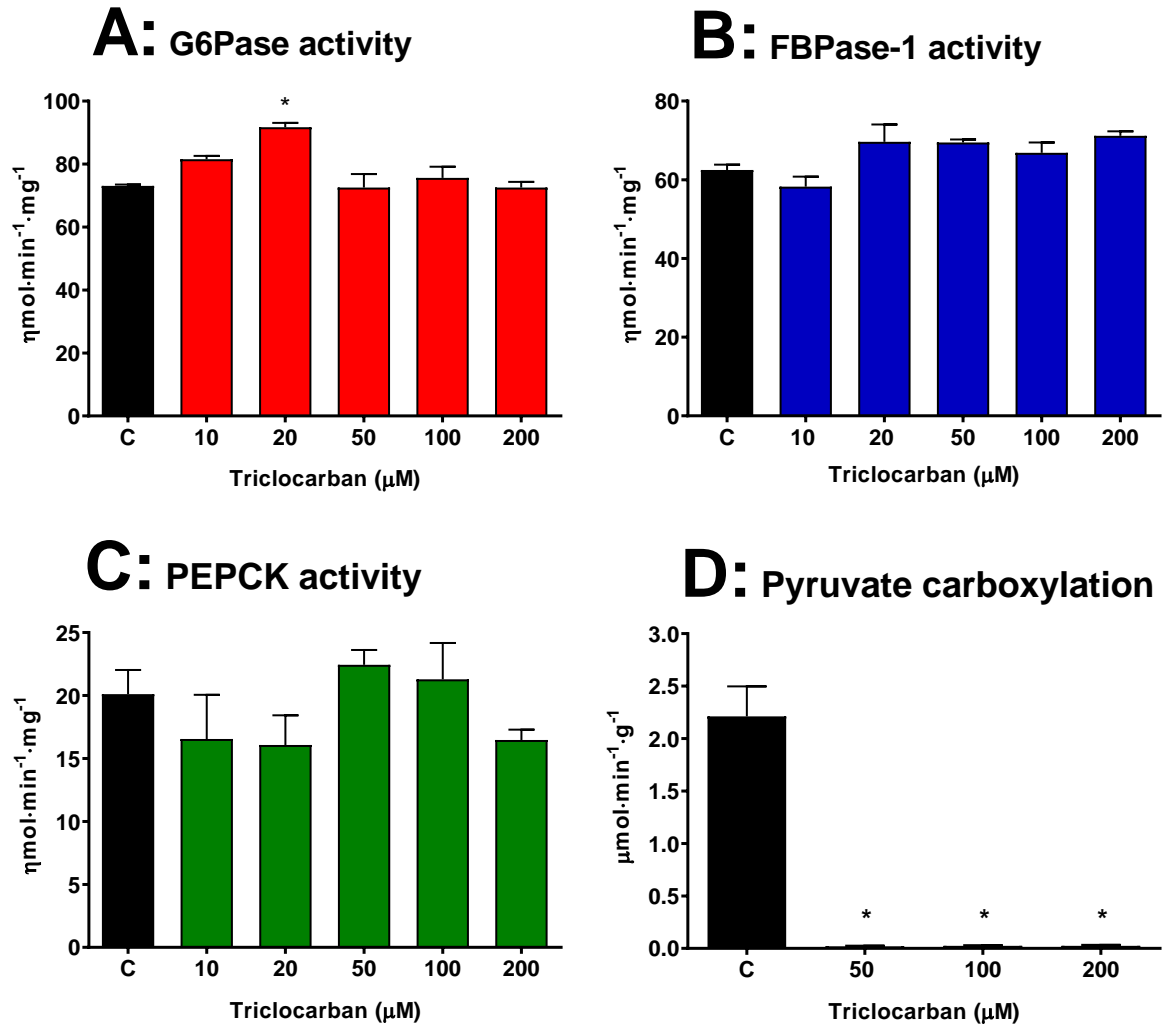


**Fig. 3**

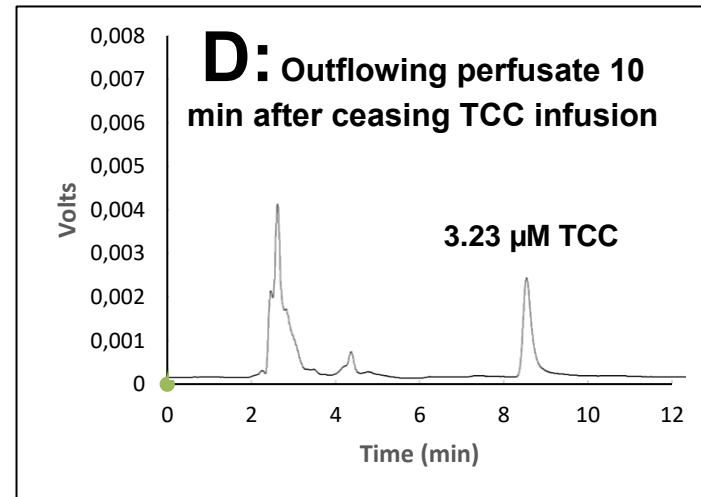
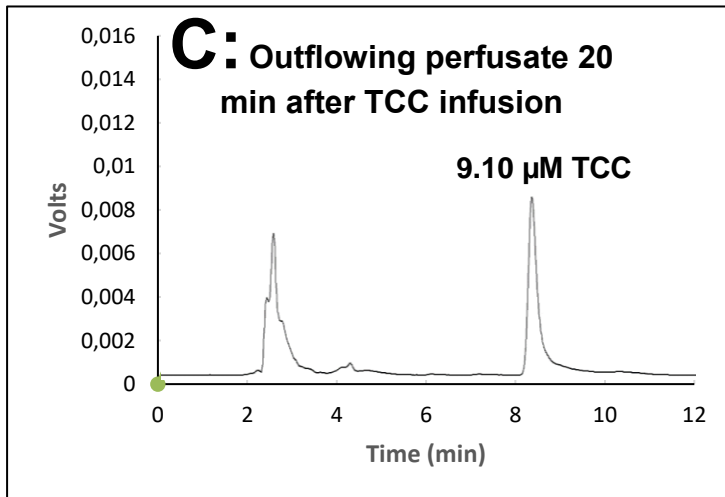
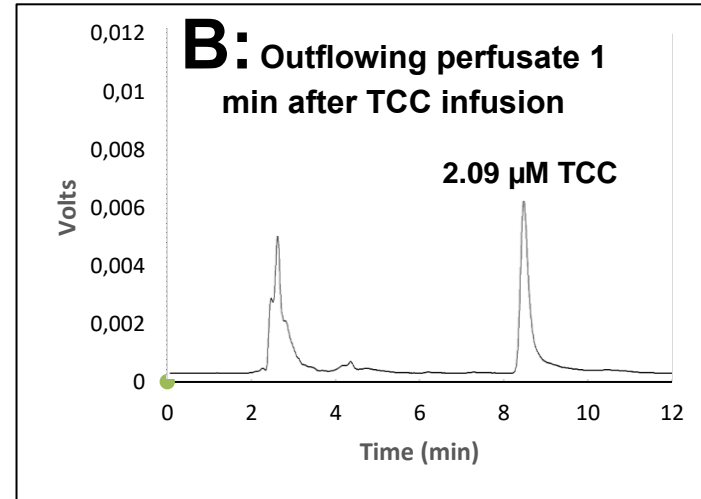
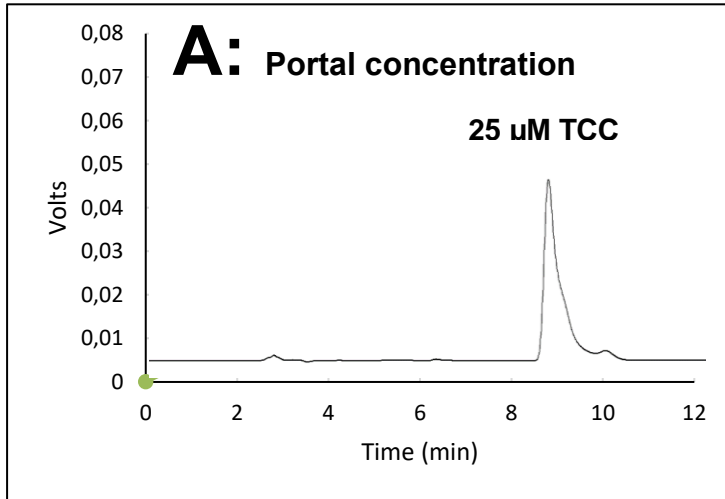


Fig. 4

